INFORMATION TO USERS

This manuscript has been reproduced from the microfilm master. UMI films the text directly from the original or copy submitted. Thus, some thesis and dissertation copies are in typewriter face, while others may be from any type of computer printer.

The quality of this reproduction is dependent upon the quality of the copy submitted. Broken or indistinct print, colored or poor quality illustrations and photographs, print bleedthrough, substandard margins, and improper alignment can adversely affect reproduction.

In the unlikely event that the author did not send UMI a complete manuscript and there are missing pages, these will be noted. Also, if unauthorized copyright material had to be removed, a note will indicate the deletion.

Oversize materials (e.g., maps, drawings, charts) are reproduced by sectioning the original, beginning at the upper left-hand corner and continuing from left to right in equal sections with small overlaps.

ProQuest Information and Learning
300 North Zeeb Road, Ann Arbor, MI 48106-1346 USA
800-521-0600

MASS TRANSFER STUDIES UNDER GAS PHASE CONTROLLED CONDITIONS

By

Chee-Chong Mah

A thesis submitted to the

Department of Chemical Engineering

University of Ottawa

In partial fulfillment of the requirements

for the degree of Master of Applied Science

December 1968

/Research Director

M. A. Sc. Candidate

TABLE OF CONTENTS

LIST OF TABLES

LIST OF FIGURES

ACKNOWLEDGMENT

The author wishes to acknowledge the guidance, patience and encouragement of Dr. J. A. Golding throughout the course of this work.

He is indebted to the Chairman of the Department, Dr. Benjamin C.-Y. Lu, for his support both moral and financial.

He also wishes to thank Mr. G. Gasperetti for his enthusiastic help in setting up the equipment and Mr. J. Auns for his assistance in obtaining photographs of the gas slugs.

Financial aid was received in the form of Natioanl Research Council Grants.

ABSTRACT

Gas-phase controlled mass-transfer for the system, hexane-nitrogen-dodecane has been studied. Three different contacting apparatuses were used: (1) a wetted wall column (2) a bubble column (3) a slug-flow absorber. The outlet gas streams from these apparatuses were analysed and the effect of gas-flow rate, liquid flow rate and contact time on overall mass-transfer efficiencies, E_T, were investigated. For the wetted wall column mass-transfer efficiencies were found to be a function of column diameter and contact time. The results are found to be consistent with the data of previous investigators. Practically no end-effect mass-transfer took place. For the bubble column, E_T was found to be very high and end-effect mass-transfer predominated. The E_E values fell between 0.98 and 0.99. E_T was observed to be the function of gas flow rate and contact time. For the slug-flow absorber, mass-transfer efficiencies were again high and end-effect mass-transfer also predominated E_E ranging from 0.94 to 0.98. E_T was observed to be the function of liquid flow rate as well as gas flow rate, and contact time. Asymtopic values of E_T less than 1.0 were observed and are considered to be as the result of incomplete liquid mixing. The effect of liquid flow rate was further studies by varying the position of liquid loading, top or bottom of the absorber. E_T values were slightly reduced when the liquid was introduced at the top of the column.

The overall gas phase mass transfer coefficients were calculated for the rise period mass-transfer. Highest values were found with the bubble column, but are considered to be low in view of the high E_T values observed. Lowest values were found with the slug flow absorber and suggested that mass-transfer

was inhibited when bubble movement is restricted. The K_{OG} values for wetted wall column, bubble column and slug-flow absorber, at 50 cc. per min. gas rate, 7 cc. per min. liquid rate and 0.5 cm. I.D. tube, were 0.15×10^{-4}, 0.35×10^{-4} and 0.029×10^{-4} g-mole/(sec.)(atm.)(cm.^{2}). respectively.

Photographs of bubbles rising in a slug-flow absorber were taken. Slug size was found to be dependent on both gas and liquid flow rate. Variations in gas and liquid rates resulted in the slugs changing in form from an elongated gas slug to a hemispherical cap.

I. INTRODUCTION

Gas-phase controlled mass transfer is an important industrial operation, for example, the absorption of soluble gases, such as ammonia, and distillation. Extensive studies of gas-phase-controlled mass transfer behaviour have been made using plant and pilot-plant sized equipment. Interaction of system variables, design variables and operating variables determine the performance of equipment and have complicated these studies, sometimes leading to conflicting results (2, 3, 7, 17).

Mass transfer in a plate column can be considered as taking place in two regions, a bubbling or clear liquid zone and a foam or froth zone. Hence, it would appear easier to study mass transfer in laboratory sized equipment where the effect of design variables can be reduced while contact time and surfaces can be determined more accurately. Due to the high mass-transfer rates observed, relatively few laboratory studies have been undertaken on gas-phase-controlled mass transfer. Most of these studies have been in wetted wall columns, where contacting conditions would not resemble those taking place in a plate column. In the laboratory investigation of mass transfer from single bubbles (22, 33), which could be expected to resemble the contacting conditions in the clear liquid zone, that have been undertaken, high end-effect mass transfer has been observed. This has considerably reduced the usefulness of these studies in determining the effect of system and operating variables on mass-transfer rates.

Only isolated studies have been made in laboratory sized equipment on mass transfer in foams (28, 38). High end-effect mass transfer has also been observed (28). It was considered

that the problem of determining the effect of mass transfer variables in a foam could be simplified by investigating mass transfer in a slug-flow absorber. Under these conditions gas slugs would be separated from each other by thin liquid films which might approximate the mass transfer conditions existing in a foam. As the first step it was decided that it would be of interest to compare mass-transfer rates under these conditions with those found in wetted wall columns and rising bubbles. Three apparatuses were then designed, (1) a bubble column, (2) a wetted wall column and (3) a slug flow absorption column, so that the three different methods of gas liquid contacting could be studied. To simplify experimental procedure the system nitrogen-hexane-dodecane was used. This allowed experiments to be carried out at ambient temperatures and permitted accurate analysis of the exit gas stream by means of a Thermal conductivity cell.

II PREVIOUS WORK

Numerous investigations involving gas-phase-controlled mass transfer have been carried out and only a brief summary is presented here: Few of the studies were concerned with laboratory sized equipment, the majority being carried out in plant or pilot-plant columns. In the laboratory sized equipment, most of the investigations studied were the evaporation of liquids in wetted-wall column with only a limited number of studies involving rising bubbles.

(a) Pilot-Plant Studies

Calderbank (7) studied gas and liquid contacting on bubble cap plate with slots varied from 1/16 in. to 1/4 in., 1 in. slot length and 2 in. cap depth. The gas flow rates varied from

20 cu.ft./min. to 80 cu.ft./min. and liquid rates were kept to the minimum necessary to provide a small overflow from the weir. Plate efficiencies obtained for the adiabatic evaporation of water and organic liquid in air were found to be substantially independent of gas loading and the type of contactor. End-effect mass-transfer was found to be high. As part of the A. I. Ch. E. research programme in the variables effecting tray efficiencies, Gerster (3) studied the mass-transfer behaviour of ammonia-air-water system using a single 24" O.D. sieve tray. Mass-transfer efficiencies were observed to be independent of gas flow rates once the critical value had been reached; below this value efficiencies decreased as gas velocities were raised. No end-effect mass-transfer was observed. Some irregular dependence of murphree vapor efficiency on superficial vapor velocity have been reported (2). These were accounted as the result of differences in design variables, system variables and operating variables. Furter (17) compared the efficiencies of bubble cap and sieve tray. The system employed was ammonia-air-water. Gas rates and liquid rates varied from 34.5 cu.ft./min. to 85.5 cu.ft./min. and 0.52 cu.ft./min. to 1.16 cu.ft./min. respectively. Both trays showed decreasing efficiencies with increasing gas flow rate at a given liquid flow rate. Efficiencies were found to increase slightly as the liquid rate was raised.

(b) Wetted Wall Column Studies

Most of the data obtained for the gas-phase controlled mass-transfer in wetted wall columns are those for vaporization of liquids (9, 19, 31, 35). The majority of the data were obtained with gas phase in turbulent flow (Reynold No. above 2500). For vapor flow rates in the laminar flow region, Gilliland (19) used the Leveque equation based on rod like or plug flow and the Gratze

equation based on parabolic velocity distribution in attempting to correlate the vapor phase mass-transfer efficiencies with the Gratze dimensionless group $W/Dv\rho N$. The best agreement for Gilliland's data and those of Haslam (27) was found to be with the Leveque equation. This has been explained by Boetler (5) on the basis of existence of density gradients giving rise to convection.

(c) Rising Bubbles Column Studies

The rate of absorption from rising bubbles to the continuous liquid phase has been found to be a function of flow rate, degree of internal circulation, surface area and contact time (6, 8, 10, 15, 25). However, due to the experimental difficulties, very few studies under the gas phase controlled condition have been carried out (7, 22). In all cases, end-effect mass-transfer has been found to be high and total efficiencies close to one hundred percent made it extremely difficult to determine the effect of variables on mass-transfer. Mass-transfer from bubbles is considered to take place in three regions, formation, rise and coalescence, as shown in Figure 1. When end-effect mass-transfer is appreciable, the mass-transfer at formation and coalescence have to be allowed for, in order to study the mechanism of mass-transfer during the rise period. This can be done by using the method devised by Hamielec (26, 30) who assumed that the end-effect mass-transfer is constant and independent of the rise period mass-transfer. Formation effect has also been studied (20, 37) using a liquid-phase controlled system. The values of E_F are very much lower than those of gas-phase controlled studies.

Extensive studies had been devoted to the mechanics of single bubbles rising from an orifice submerged in a liquid e.g.(13). These studies have found that at gas velocities up to 6.5 cc./sec.,

WETTED WALL COLUMN

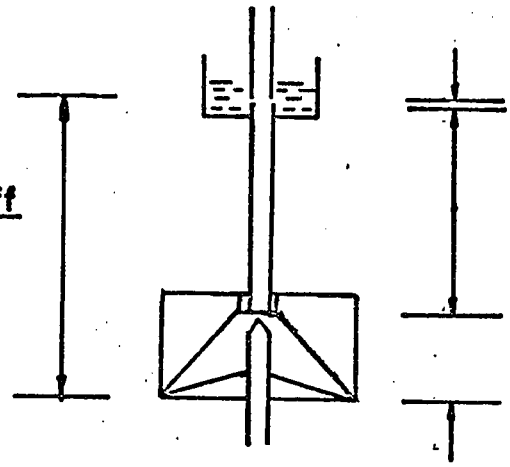

$$E_T = \frac{y_{on} - y_{off}}{y_{on} - y^*}$$

$$E_C = \frac{y_2 - y_{off}}{y_2 - y^*}$$

$$E_S = \frac{y_1 - y_2}{y_1 - y^*}$$

$$E_F = \frac{y_{on} - y_1}{y_{on} - y^*}$$

BUBBLE COLUMN

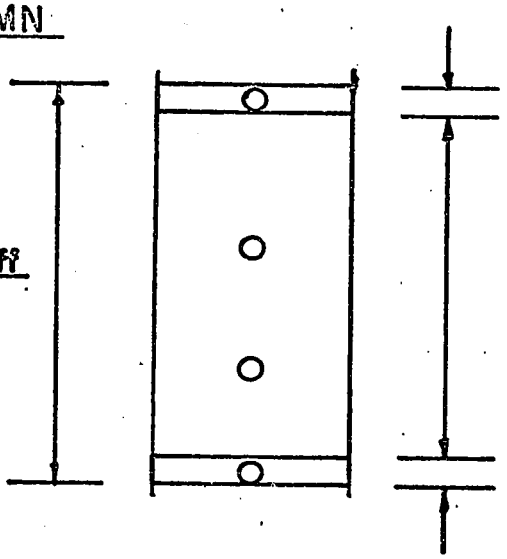

$$E_T = \frac{y_{on} - y_{off}}{y_{on} - y^*}$$

$$E_C = \frac{y_2 - y_{off}}{y_2 - y^*}$$

$$E_S = \frac{y_1 - y_2}{y_1 - y^*}$$

$$E_F = \frac{y_{on} - y_1}{y_{on} - y^*}$$

SLUG FLOW ABSORBER

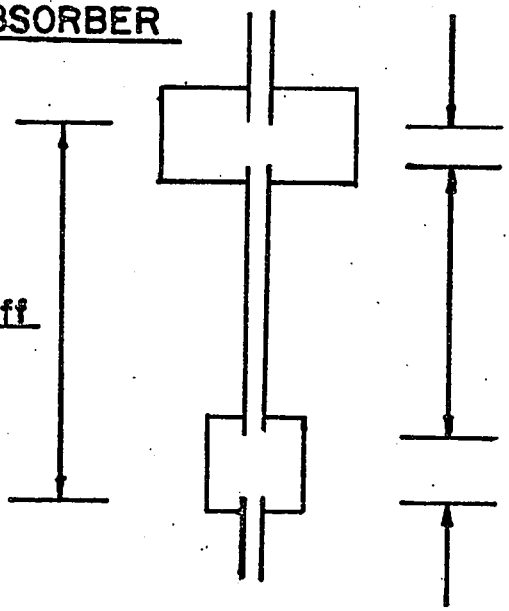

$$E_T = \frac{y_{on} - y_{off}}{y_{on} - y^*}$$

$$E_C = \frac{y_2 - y_{off}}{y_2 - y}$$

$$E_S = \frac{y_1 - y_2}{y_1 - y^*}$$

$$E_F = \frac{y_{on} - y_1}{y_{on} - y^*}$$

the volume of the bubble and the diameter of the orifice were in a constant ratio, $\frac{V}{D} = 0.330$, while at higher gas velocities, the relationship becomes $\frac{V}{D} = \frac{\pi}{\rho} \frac{\sigma}{g}$. In both cases, the bubble shape and velocity were influenced by the liquid viscosity, surface tension and wall effect. The influence of viscosity and surface tension on bubble formation has been studied by Schnurmann (34) and Halberstadt and Prausnitz (25). It was found that surface tension rather than viscosity was the property determining bubble size. Hobler (32) after a review of previous studies, has introduced a method for the approximate calculation of the surface area rise, velocity and contact time for the rising bubbles in the column.

III THEORETICAL

The fractional approach of the vapor stream to equilibrium with the liquid phase is generally expressed in terms of an overall gas phase efficiency, E_T, where $E_T = \frac{y_{on} - y_{off}}{y_{on} - y^*}$ y_{on} = mole fraction of soluble component in inlet gas, y_{off} = mole fraction of soluble component in outlet gas, and y^* = mole fraction of soluble component in the gas phase that would be in equilibrium with the liquid phase.

The equations relating the overall mass-transfer efficiencies to the contacting length and contact time for the three gas-liquid contacting methods can be derived as given below. As this was a exploratory study, only simple models were used.

(a) Wetted wall column

The rate of absorption of hexane from the bulk of the gas to the liquid phase can be expressed by the following differential equation, where gas phase is assumed perfectly mixed horizontally.

$$G\,dy = - \frac{K_{OG}}{\phi} P\,(y - y^*).dA. \quad \ldots\ldots \quad (1)$$

where

K_{OG} = gas phase mass-transfer coefficient, $\frac{\text{g-mole}}{(\text{cm.}^2)\,(\text{sec.})\,(\text{atm.})}$

y = mole fraction of hexane in gas phase

P = total pressure $\approx$ 1 atmosphere.

ϕ = relative velocity factor ≈ 1 (Lean gas)

G = constant molal gas flow rate, g-mole/sec. (Lean gas)

A = contacting area of the two phases.

Equation (1) can be further written in another form

$$G\,dy = -K_{OG}\,P\,(y - y^*)\,d\,(2\pi r Z) \quad \ldots\ldots\ldots \quad (2)$$

where

r = (tube diameter minus twice the film thickness of the liquid.) x 1/2

Z = tube length, cm.

Rearranging and integrating the R. H. S. and L. H. S.

$$\int_{y_1}^{y_2} \frac{dy}{y - y^*} = -\int_0^Z \frac{K_{OG}\,P}{G}\,2\pi r\,dZ = -\frac{K_{OG}\,P}{G}\,2\pi r\,Z \quad (3)$$

Where y_1 and y_2 are the mole fraction of hexane in the gas stream at the inlet and outlet of the mass-transfer section.

As y^* is a function of the concentration of hexane in the liquid phase, it may change as the gas phase composition goes from y_1 to y_2. The variation must be known before the L. H. S. can be integrated. However, at high liquid rates, y^* can be maintained constant and only depend on the concentration of hexane in inlet liquid. Making this assumption, equation (3) becomes

$$\ln \frac{y_1 - y^*}{y_2 - y^*} = \frac{K_{OG} P}{G} 2\pi r Z \quad \ldots\ldots\ldots \quad (4)$$

Equation (4) can be rearranged to give:

$$- \ln (1 - E_S) = \frac{K_{OG} P}{G} 2\pi r Z \quad \ldots\ldots\ldots \quad (5)$$

Where E_S is the mass-transfer efficiency during the rising period.

Finally, if Z is replaced by $V\Theta$, where V is the average gas velocity of the gas phase and Θ, the contact time, the following equation can be obtained:

$$- \ln (1 - E_S) = \frac{K_{OG}}{G} P \quad 2\pi r \; V\Theta \quad \ldots\ldots \quad (6)$$

(b) Rising Bubbles Column

A similar equation can be derived for the steady state mass-transfer from rising bubbles. The rate equation of absorption is given by:

$$\frac{G\, dy}{d\Theta} = -K_{OG} P (y - y^*) Af \quad \ldots\ldots\ldots \quad (7)$$

where

G = molal gas flow rate, g-mole/sec.

A = surface area of a bubble, $cm.^2$

Θ = contact time, sec.

f = frequency, bubbles/sec.

Proceeding as before, the final following equation can be obtained:

$$- \ln (1 - E_S) = \frac{K_{OG} PAf}{G} \Theta \quad \ldots\ldots\ldots \quad (8)$$

(c) Slug Flow Absorber

An analogous equation can be derived for the rate of absorption in slug flow absorber, that is,

$$\ln (1 - E_S) = \frac{-K_{OG}\ Pf_S}{G}\ A_S\ \Theta \qquad \ldots\ldots\ (9)$$

where

f_S = frequency, slugs/sec.

A_S = surface area of the slug

For the three above equations, the plot of $-\ln (1 - E_S)$ versus seal height or contact time should give a straight line passing through the origin and enable the overall mass-transfer coefficient to be evaluated from the slope of this straight line.

(d) End Effects

In practice, however, only E_T can be measured and E_T and E_S are not equal when end-effect mass-transfer takes place. End effect mass-transfer is mass-transfer taking place at formation and coalescence periods, in bubble and slug flow columns. In the wetted wall column, gas and liquid flow disturbances can occur at the inlet and after the outlet section of the mass-transfer column and may lead to increased rates of mass-transfer. The mass-transfer zones for the three contacting apparatus are shown in Figure 1. Previous invesitgations have shown that when the end-effects were high (22, 33), they should be taken into consideration. The method developed by Hamielec (26, 30) permitted end-effects to be allowed for. In this method, the end-effect mass-transfer was assumed constant, that is, independent of rise period. Then for constant y^*, the following relationship can be obtained:

$$\ln (1 - E_S) = \ln (1 - E_T) - \ln (1 - E_E) \qquad (9)$$

If equation (9) is substituted into equation (6), (8) and (9), they can be rearranged as:

$$-\ln(1 - E_T) = \frac{K_{OG} P}{G} \quad 2\pi r V\Theta \quad - \ln(1 - E_E) \quad \ldots \quad (10)$$

$$-\ln(1 - E_T) = \frac{K_{OG} PAf}{G} \quad \Theta \; - \; \ln(1 - E_E) \quad \ldots\ldots\ldots \quad (11)$$

and

$$-\ln(1 - E_T) = \frac{K_{OG} PA_S}{G} f_S \; \Theta \; - \; \ln(1 - E_E) \quad \ldots\ldots \quad (12)$$

A plot of $-\ln(1 - E_T)$ against contact time for each equation should accordingly yield a straight line from which K_{OG} and E_E can be evaluated from the slope and ordinate intercept of the curves at $\Theta = O$ respectively.

IV EXPERIMENTAL

(a) Apparatus

A schematic diagram of the apparatus is shown in Figure 2. Nitrogen from the nitrogen cylinder was saturated with hexane by passing the nitrogen through four saturators, immersed in cooling baths as shown (7) and (8). The first water bath was kept at ambient temperature while the second methanol-water bath was maintained at -4° C. This gave practically constant inlet gas composition, which was calculated assuming gas ideality and equal to $\frac{\text{vapor pressure of hexane}}{\text{total pressure}}$. Before entering the saturators, the nitrogen flow rate was measured by a rotameter (2) and the nitrogen was also passed through the reference side of the T. C. cell. After the saturators the nitrogen-hexane mixture entered the absorber (9), where mass-transfer took place. The liquid dodecane was pumped from a head tank (10) by means of a micrometer pump. The dodecane was cooled and pulsations damped (13) before the liquid was fed into the

1. Nitrogen Cylinder
2. Rotameter
3. Pressure Regulator
4. Flow Controller
5. Manometer
6. T. C. Cell
7. Saturator at Room Temperature
8. Saturator at -4° C Temperature
9. Mass Transfer Column
10. Dodecane Head Tank
11. Micrometer Pump
12. Cooling Water Bath
13. Pulsation Dampener
14. Dodecane Receiver

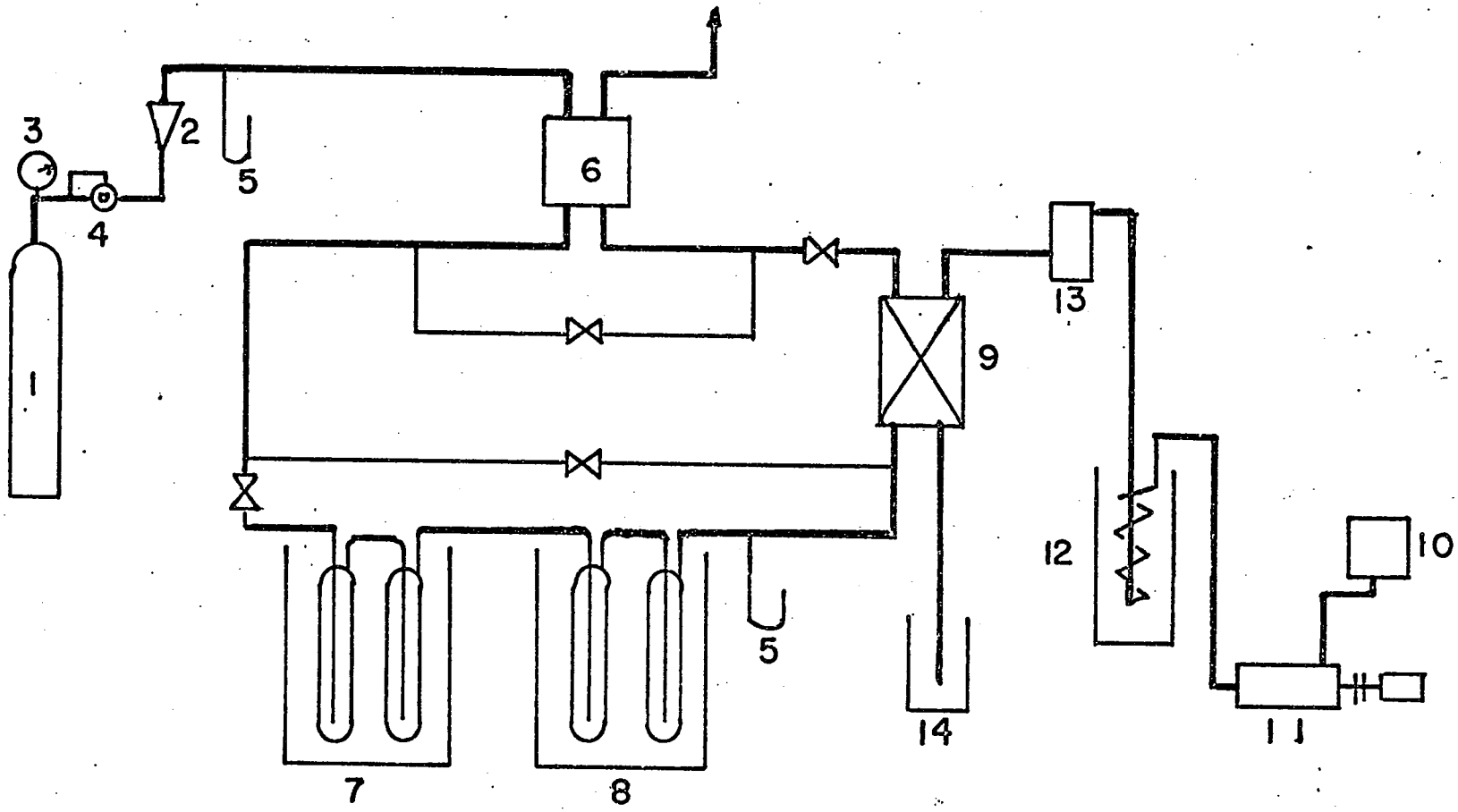

Figure 2: Schematic Diagram of Apparatus

absorber. The outlet gas stream then returned to the T. C. cell for analysis while outlet liquid was collected in a receiver (14).

(b) Equipment Details

1) Saturator

The saturators comprised a series of four 1" I.D. and 10" long gas bubblers fitted with sintered glass disks as shown in Figure 3. They were maintained 4/5 full of hexane.

2) Dodecane Feed

The dodecane feed was maintained constant by means of a MILROYAL D CONTROLLED VOLUME PUMP of MILTON ROY COMPANY, ST. PETERSBURG, FLORIDA. Before entering the mass-transfer column, the dodecane was cooled to 20° C. by pumping the liquid through a coil immersed in a water bath held at about 18° C.

3) Wetted Wall Column

The wetted wall column shown in Figure 4 was made up of a known length of glass tubing fitting in to the inlet and outlet sections (2) and (6). The contacting of the gas and liquid took place countercurrently with hexane-nitrogen mixture entering the bottom of the column and dodecane at the top of the column. Two different diameter tubes of 0.4 cm. and 0.5 cm. were studied with the length being varied from 3 to 13 cm.

4) Bubble Column

The bubble column was made up of a glass column, 10 cm. I.D. and 25 cm. in length, mounted on a brass plate as shown in Figure 5. A 0.1 cm. I.D. orifice of about 1" long was connected to the gas inlet at the bottom of the column. A bubble breaker was attached to an inverted

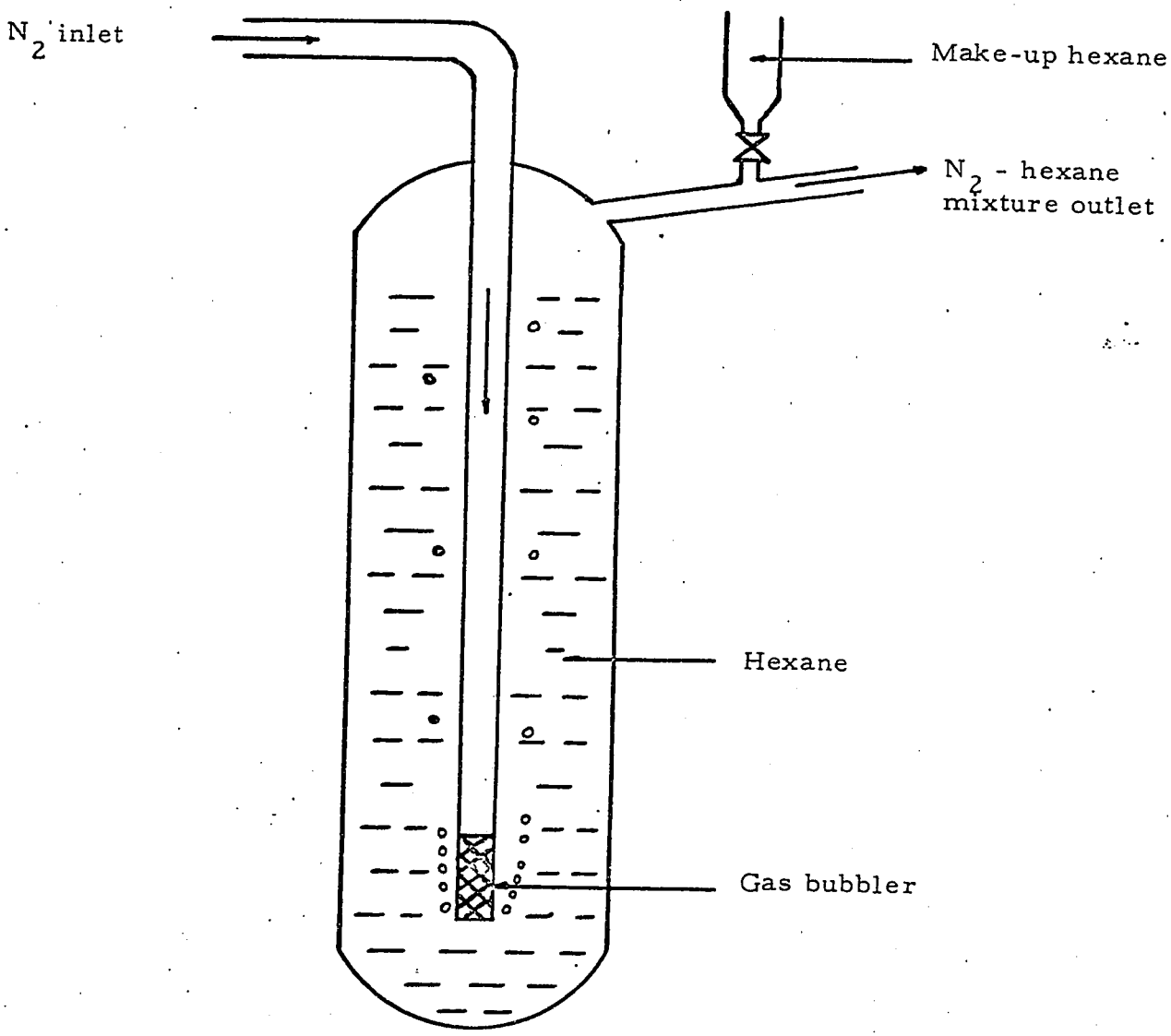

Figure 3: Hexane Saturator

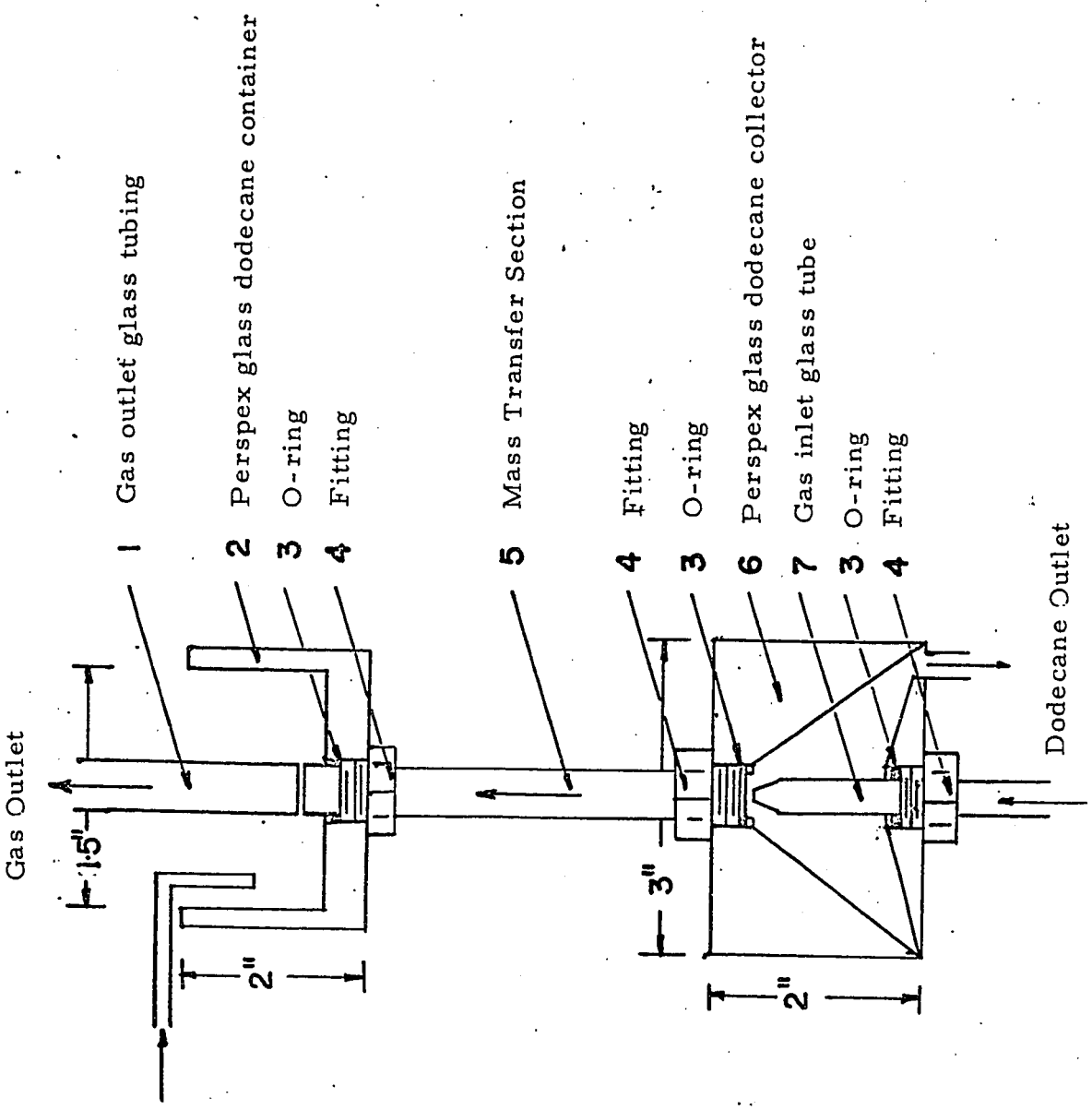

Figure 4: Wetted Wall Column

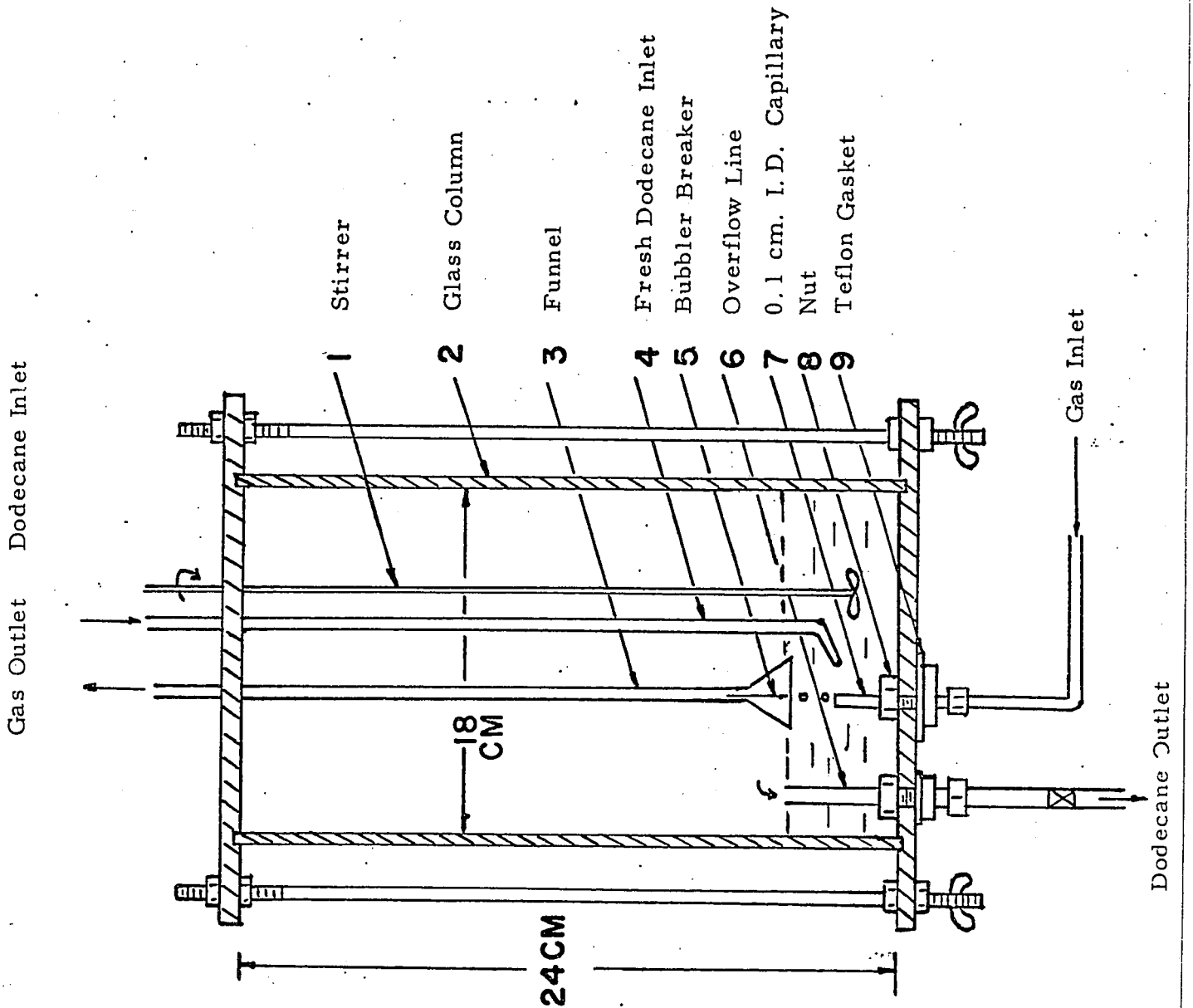

Figure 5: Bubble Column

funnel and positioned as shown in the figure 5 . The depth of the liquid in the column was varied by changing the length of the overflow line.

5) Slug-Flow Absorber

The slug-flow absorber was similar to the wetted wall column. They were made up of known lengths of glass tubing fitting into the upper and lower section of the absorber as shown in Figure 6. Two absorbers were used to determine the effect of the position of liquid loading on mass-transfer in slug flow. The liquid was fed either at the top or bottom of absorption column. Slug flow was induced by positioning the inlet gas nozzle.

A needle was again used as a bubble breaker (4) to minimize the end-effect mass-transfer in the outlet section. Three different diameters of tubing, 0.4, 0.5 and 0.6 cm. respectively were used while the length was varied from 3 to 14 cm.

(c) Procedure

1) Gas Analysis

The composition of hexane in the gas flow was analysed with a Thermal conductivity cell and potentiometer. The electrical circuit for the cell and other auxiliaries is shown in Figure 7.

The T. C. cell was maintained at a constant temperature of 30° C ± 1° by being placed in an insulated aluminum container. The inside of the container was heated by means of a heating tape and power supply to the tape was controlled manually with a power-stat . The current supply to the T. C. cell was from a power supply controller unit obtained from Gow Max Company. The potentiometer employed was

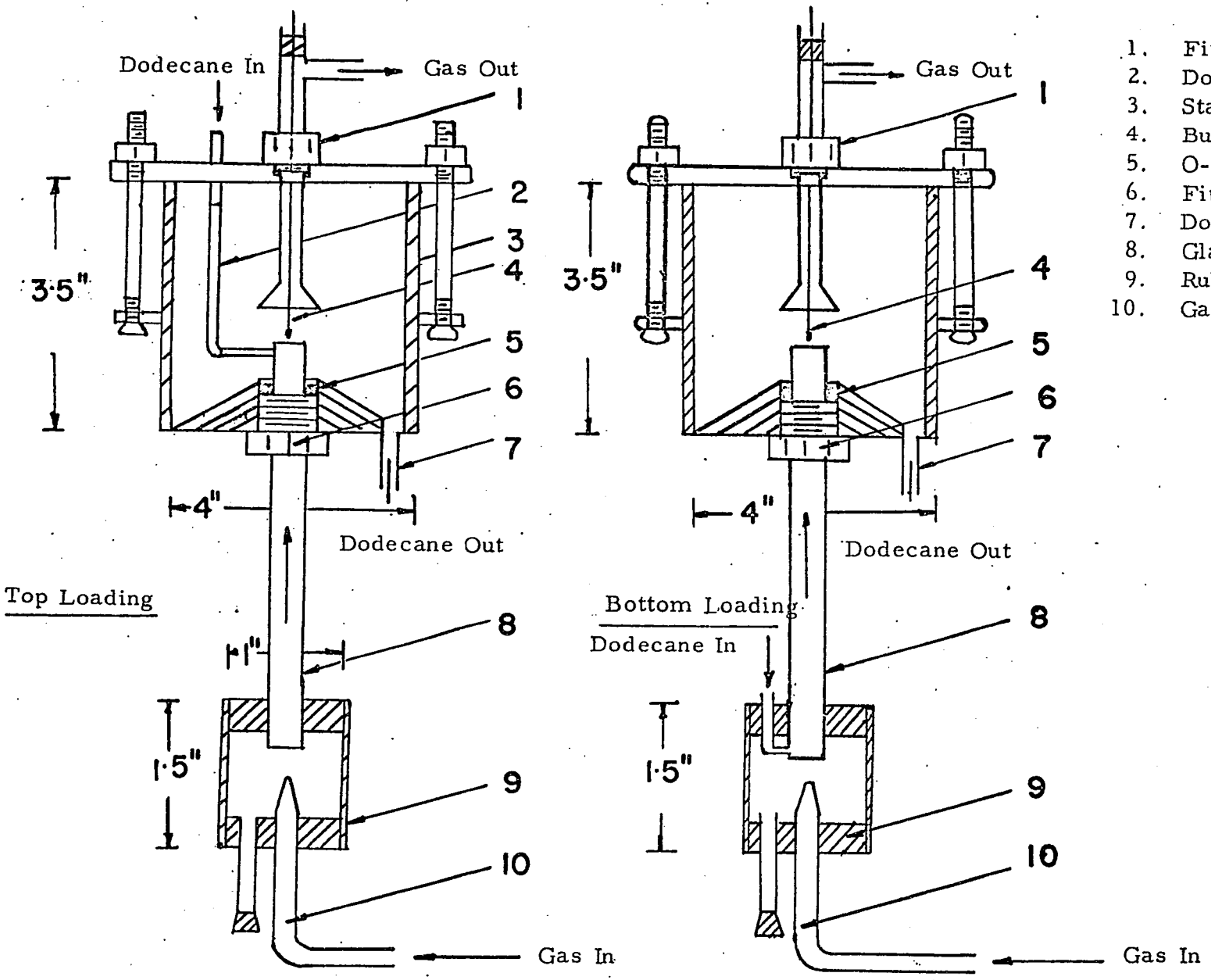

1. Fitting
2. Dodecane Inlet
3. Stainless steel box
4. Bubble Breaker
5. O-ring
6. Fitting
7. Dodecane Outlet
8. Glass Tubing
9. Rubber Stopper
10. Gas Inlet

Figure 6: Slug Flow Absorber

Figure 7: Electrical Wiring T. C. Cell

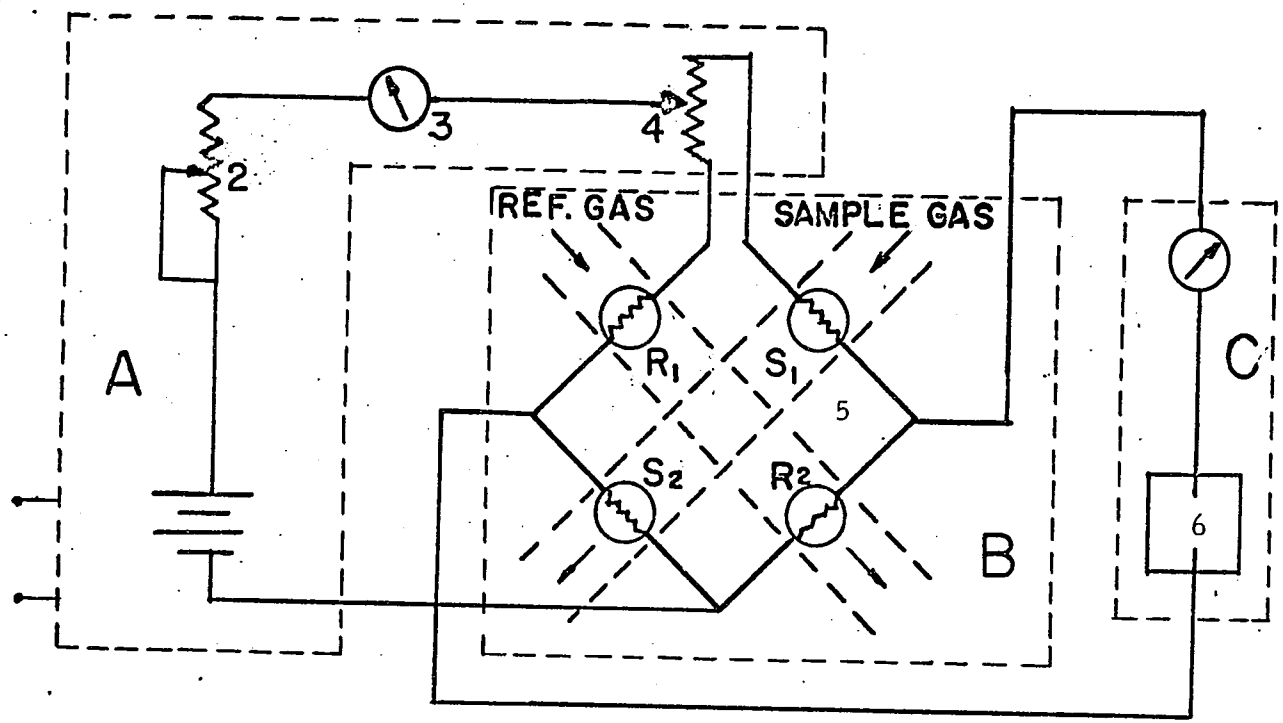

1. 12 volts power supply
2. Resistance 50 ohms
3. Milliameter
4. Resistance 2 ohms
5. T. C. cell
6. Potentiometer

R_1-R_2, S_1-S_2: Filament pairs

Parts A, B and C inside dashed line were included in Power Supply Controller Unit, T. C. cell and Potentiometer

of model no. 3184 D and able to give a smallest M. V. reading of 0.01 M. V.

The cell was calibrated by passing nitrogen-hexane gas mixture of a known composition through one side of the cell and pure nitrogen through the reference side of the cell and measuring the cell unbalance with the potentiometer. The saturator gas mixture were prepared by bubbling nitrogen through liquid hexane as has been described previously. The variation in composition was achieved by changing the temperature of the second water bath.

The cell unbalance was found to be a function of the current passing through the cell as shown in Figure 8. The maximum deflection was observed at 150 M. A. but initially it was found only possible to maintain the current at 125 ma. when the power supply to the T. C. cell was from the 12 volt battery. This was due to the manual potentiometer (2) not being sufficiently accurate to control the current at 150 ma. Then, after the power supply was changed, it was decided to keep the cell current of 125 ma for the remaining runs.

Gas flow rate was found to have virtually no effect on the cell unbalance and the calibration curve is shown in Figure 9.

A gas mixture was tested for saturation by condensing hexane in the gas in a dry ice trap. The test showed that the mixture was 99% saturated with hexane. Further, nitrogen was bubbled through dodecane at 20° C, 25° C and 27° C and the cell unbalance was found to be negligible.

2) Experimental Procedure

At the start of a run, nitrogen was first passed through the

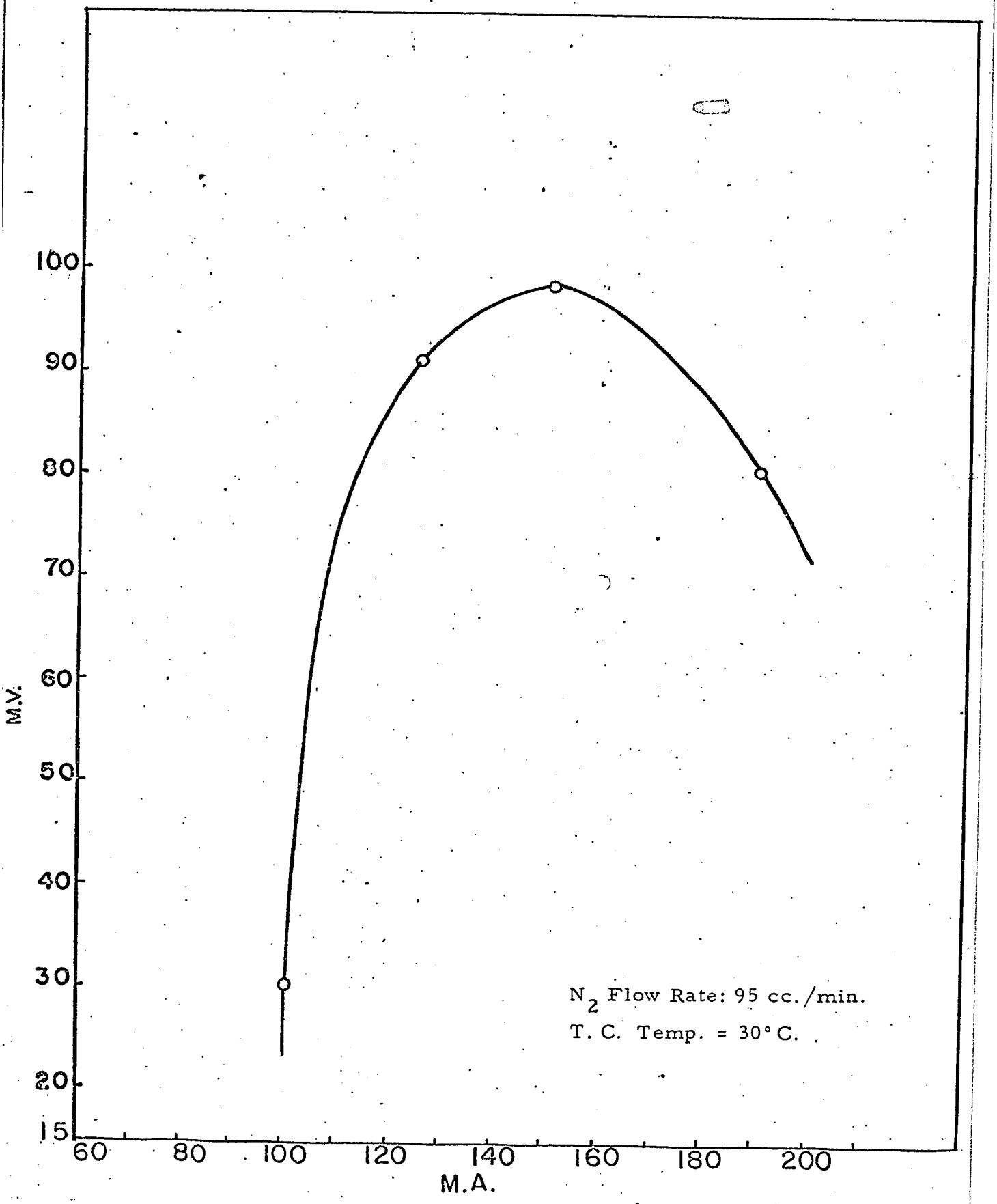
100
90
80
70
60
50
40
30
20
15
M.V.
60
80
100
120
140
160
180
200
M.A.
N_2 Flow Rate: 95 cc./min.
T. C. Temp. = 30° C.

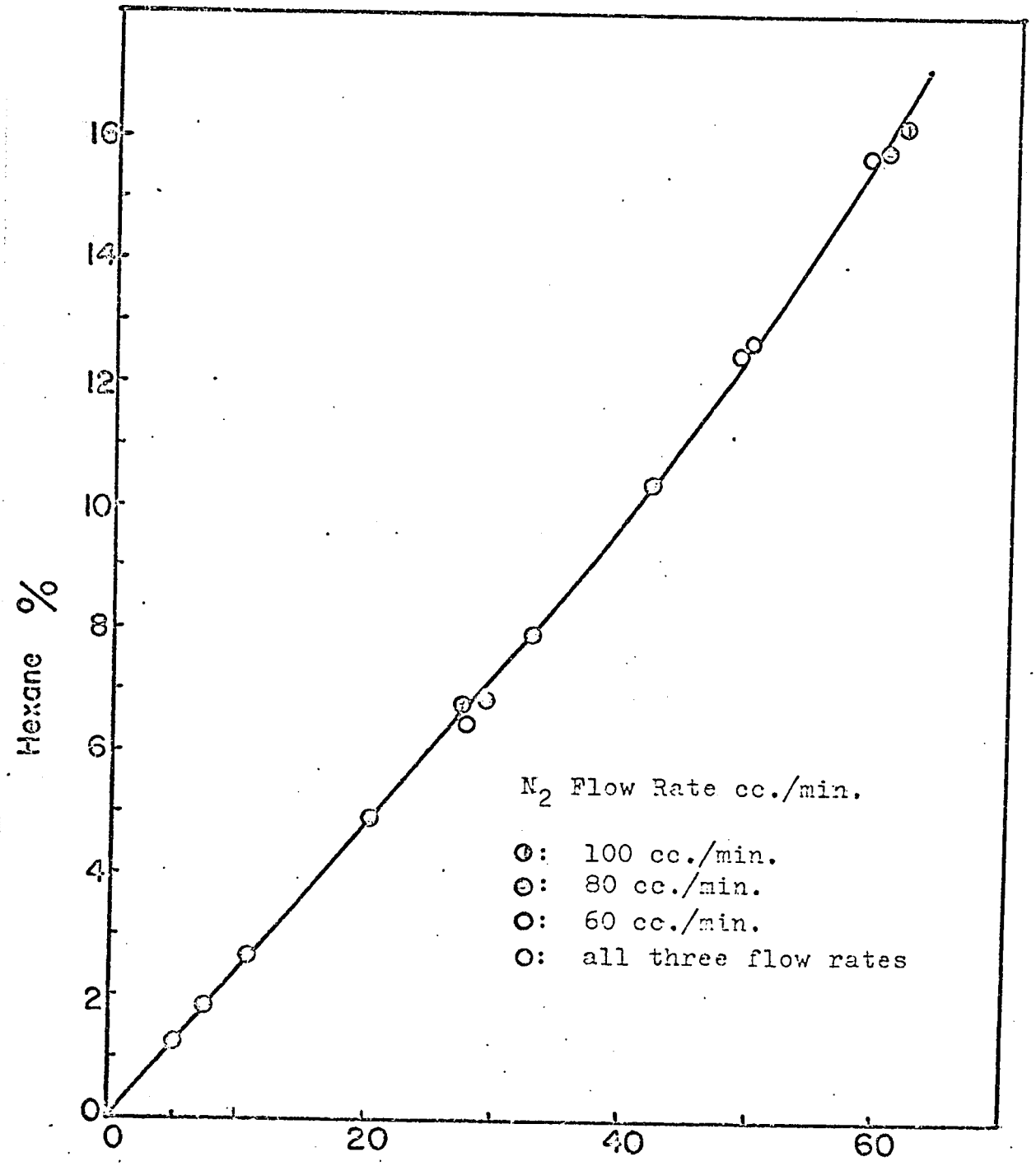

Fig.9 Calibration Curve of T.C.Cell

absorption and the T. C. cell at a known rate, using the by-pass as shown in Figure 2. The dodecane flow was then started, T. C. cell checked and potentiometer adjusted to give zero deflection if necessary. Then, the nitrogen was passed into the saturators and into the absorber where mass-transfer took place. In the case of the bubble column, the liquid was brought to the desired level before the introduction of hexane saturated gas mixture from the saturator. The outlet gas composition was determined by noting the T. C. cell unbalance and allowing it to reach steady state. After Steady state had been reached, the M. V. reading, nitrogen and dodecane flow rates were recorded together with barometric pressure and room temperature. The dodecane feed was stopped and the nitrogen stream diverted back to the by-pass line. A duplicate run was then carried out by repeating the procedure. A series of runs were carried out for each contacting length or seal height at different gas rates, liquid rates and inside tube diameters.

V RESULTS AND DISCUSSION

(a) Introduction

Overall efficiency data were obtained for the absorption of hexane from nitrogen carrier gas in the three different gas-liquid contacting apparatuses.The gas rates employed varied from 50 to 100 cc. per min. while the liquid rates were varied from 2 to 9 cc. per min. Contact times were varied by changing either the liquid seal height or the length of the absorber. Each experimental run was carried out in duplicate and the mean values are shown in the figures. In addition, flow characteristics in the slug flow absorber were observed photographically. The data obtained are given in Appendix I and overall efficiency data are shown in Figures (10, 11, 13-A, 14, 15, 17, 18).

(b) Wetted Wall Column

The flows, both the liquid, as thin film flowing down the inside surface of the tube and gas flow rising up the tube, were found to be laminar. Reynold numbers of flows were from 17 to 43 for gas and 17-26 for liquid.

The overall efficiency data obtained are shown in Figure 10 and 11. The figures show that E_T increased with increasing contacting length but decreased as the gas flow rates and column diameters were increased. In addition, as expected, liquid flow rate was found to have virtually no effect on E_T. The plot of $-\ln (1 - E_T)$ against contact time, Θ, showed that, under the condition studied, very little, if any, end effect mass-transfer was taking place, and all the straight line have been drawn to pass through the origin at $\Theta = 0$. The mass-transfer coefficient were calculated from the slope of the straight lines using equation (10) and are tabulated

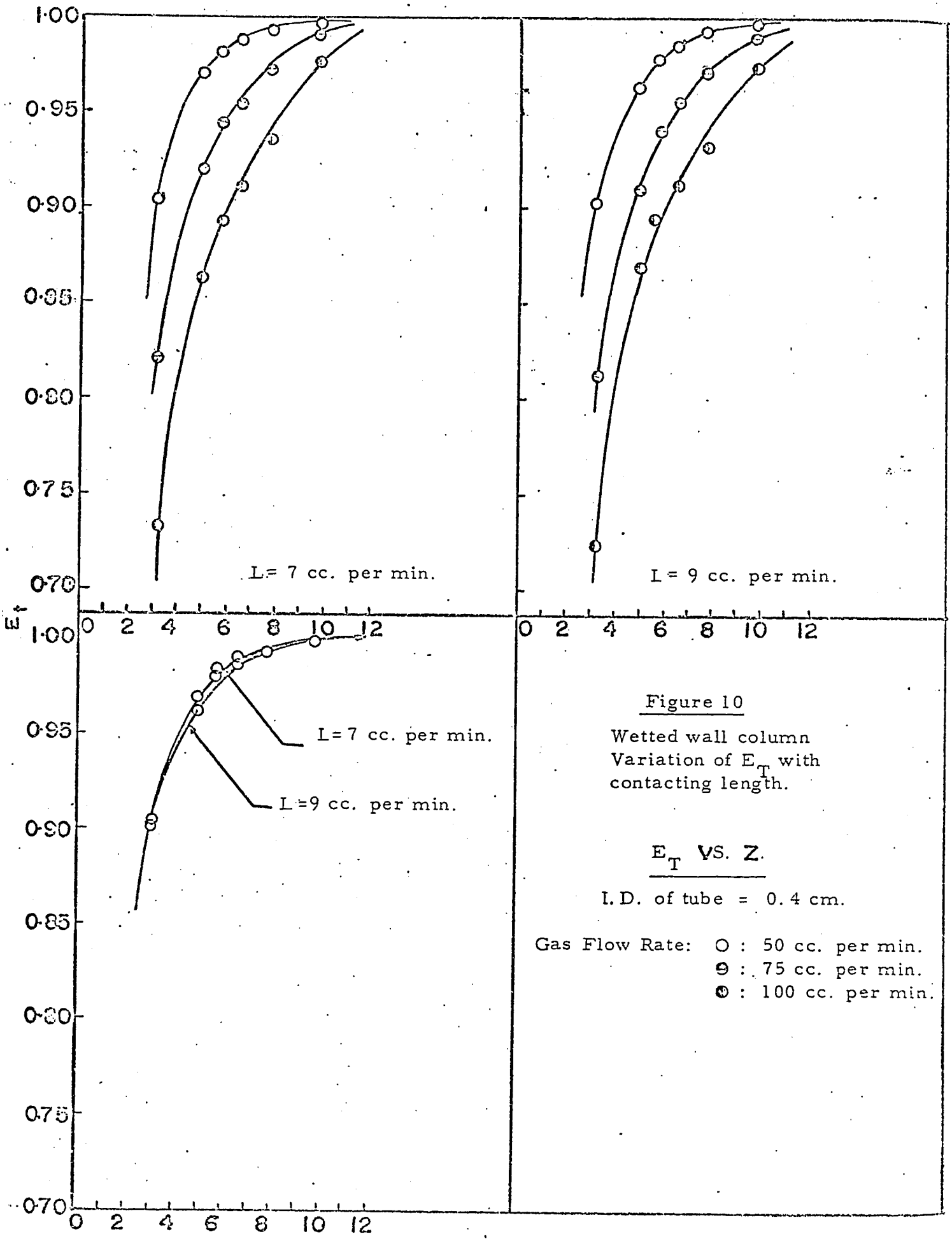

Figure 10

Wetted wall column
Variation of E_T with contacting length.

E_T VS. Z.

I. D. of tube = 0. 4 cm.

Gas Flow Rate: O : 50 cc. per min.
⊖ : 75 cc. per min.
● : 100 cc. per min.

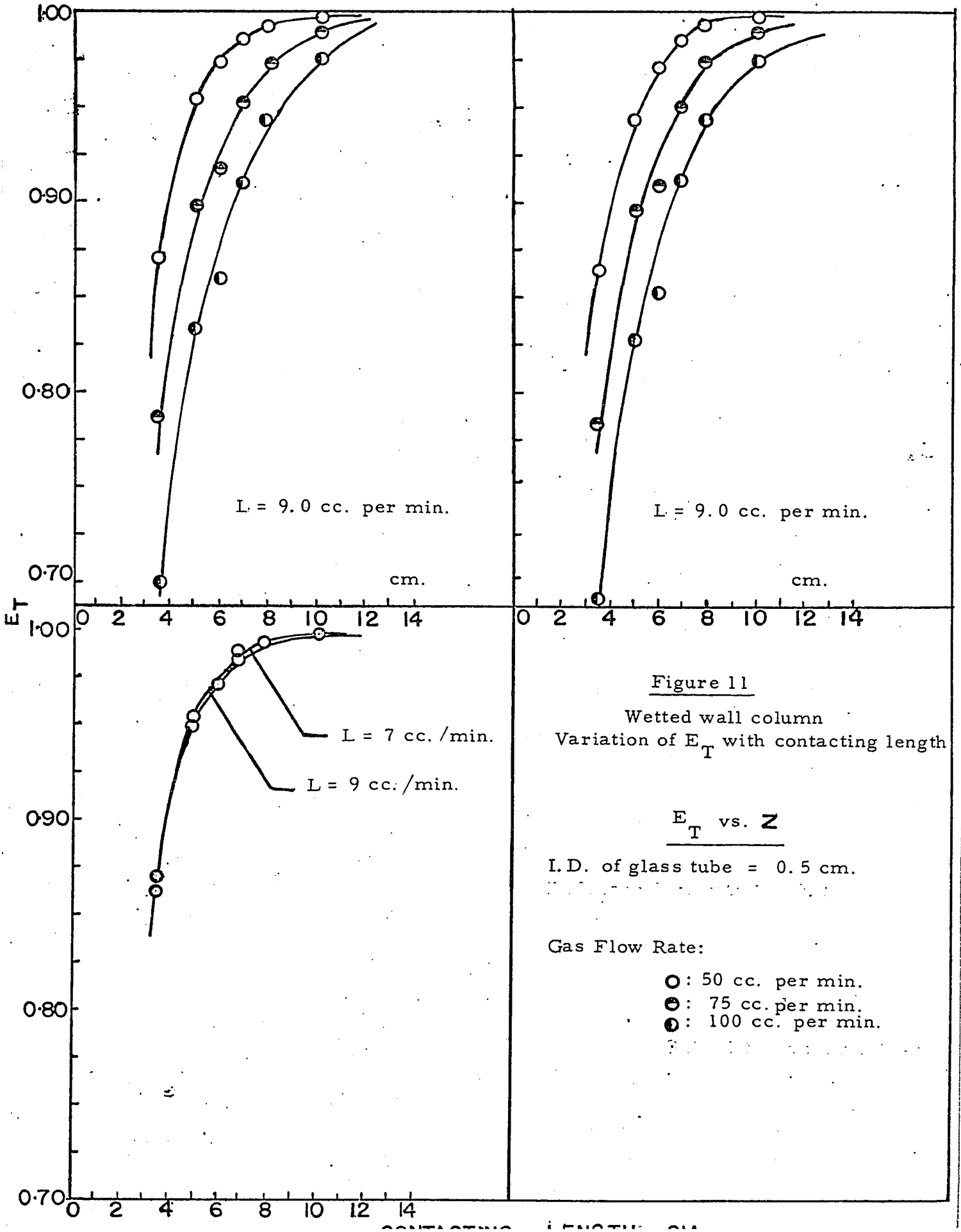

Figure 11

Wetted wall column
Variation of E_T with contacting length

E_T vs. Z

I.D. of glass tube = 0.5 cm.

Gas Flow Rate:

○ : 50 cc. per min.
◔ : 75 cc. per min.
◑ : 100 cc. per min.

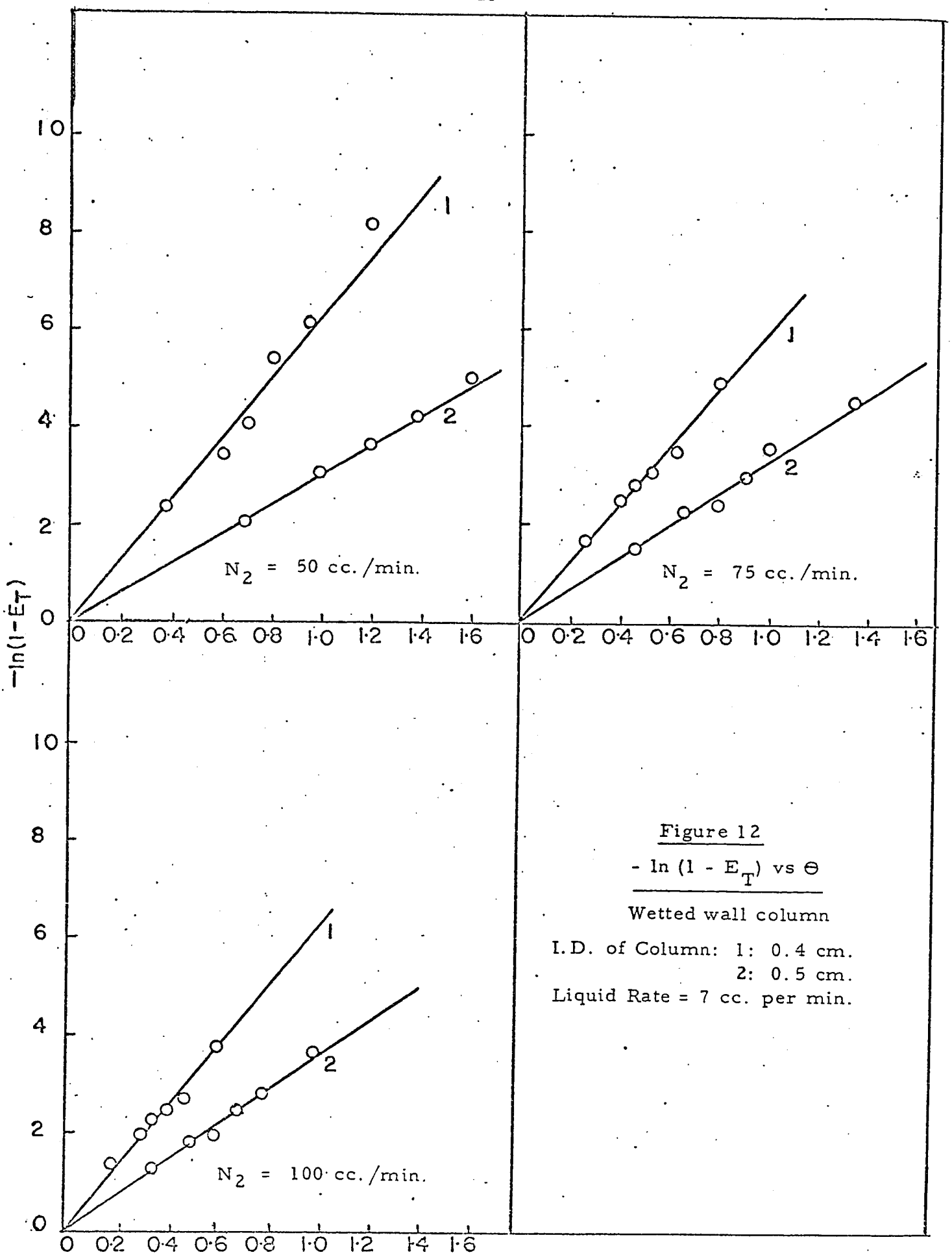

Figure 12

$-\ln(1 - E_T)$ vs Θ

Wetted wall column

I.D. of Column: 1: 0.4 cm.
2: 0.5 cm.

Liquid Rate = 7 cc. per min.

Mass Transfer Coefficient, K_{OG}

N_2 cc./min.	I.D. of tube cm.	K_{OG} (g-mole/sec. atm. cm.^{2}) x 10^4
50	0.4	0.24
75	0.4	0.22
100	0.4	0.23
50	0.5	0.15
75	0.5	0.16
100	0.5	0.17

K_{OG} decreased as the tube diameter increased and was not a function of the gas flow rate for the 0.4 cm. tube as predicted by equation (10). For the 0.5 cm. tube, K_{OG} slightly depended on the gas flow rate and this could have been caused by the incomplete wetting of the surface of the tube or the occurence of ripples at the gas-liquid interface, but no further studies were made. The same trend was observed when the data were compared with those reported in the literature for the absorption of ammonia at the similar Reynold numbers by Haslem, Hers-key and Keen (27). The data, when they were all plotted as E_T against $\frac{W}{\rho D_v N}$ as suggested by Sherwood (19), were scattered below the curves predicted by Leveque and Gratze equations.

(c) Bubble Column

These results were characterised by high mass-transfer efficiencies as shown in Figure 13. The efficiencies were found to be almost one hundred per cent in all cases. They decreased slightly as the gas flow rate was increased. Plots of $-\ln(1-E_T)$ versus contact time, Θ, are shown in Figure 13-B. Straight lines drawn through the points show that end effect mass-transfer in every case accounted for the majority of the mass-transfer

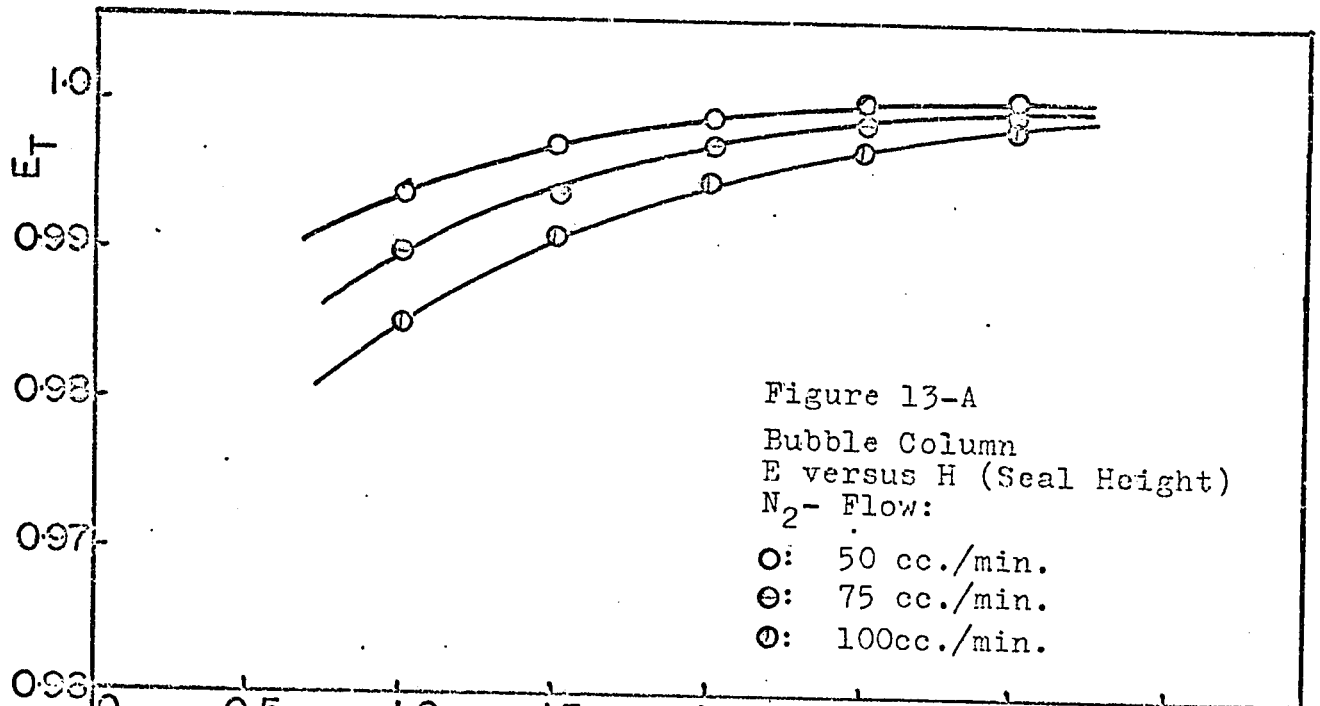

Figure 13-A

Bubble Column
E versus H (Seal Height)
N_2- Flow:
O: 50 cc./min.
Θ: 75 cc./min.
Φ: 100cc./min.

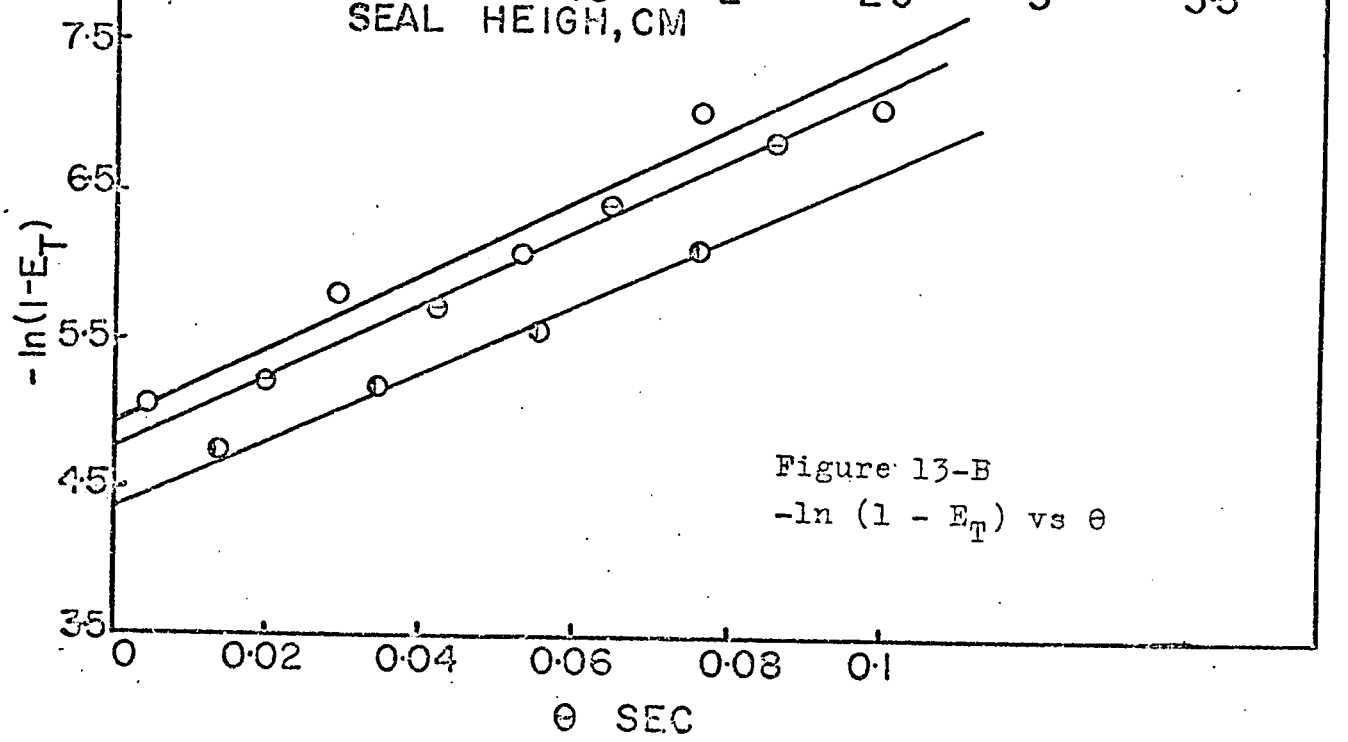

Figure 13-B
$-\ln (1 - E_T)$ vs θ

taking place. Their values are tabulated as:

N_2 - Flow cc./min.	End Effect, E_E
50	0.9930
75	0.9918
100	0.9834

The contact time, Θ, was evaluated from the correlation reported by Hobler (32) for chain bubbling conditions. Mass transfer coefficients, K_{OG}, were evaluated from the slope of the straight lines, assuming uniformity of bubble size, constant rise velocity and bubble diameter which were calculated from the equations given by Hobler (32), see appendix (II).

Mass Transfer Coefficient, K_{OG},

N_2 - Flow cc./min.	K_{OG} g-mole/(sec.)(atm)($cm.^2$) $\times 10^4$
50	0.55
75	0.63
100	0.71

These values are higher than those found with the wetted wall column and increased as the gas flow rate was increased. However, the rise period covers such a small section of the total efficiencies measured that no real conclusion can be drawn.

(d) Slug Flow Absorber

(I) Bottom Loading

The data obtained are shown in Figure 14 and 15. Mass transfer efficiencies were again high, depended on gas flow rate, contact time, tube diameter and liquid flow rate. E_T increased with increase in tube diameter or contact time but fell as the gas velocity was increased.

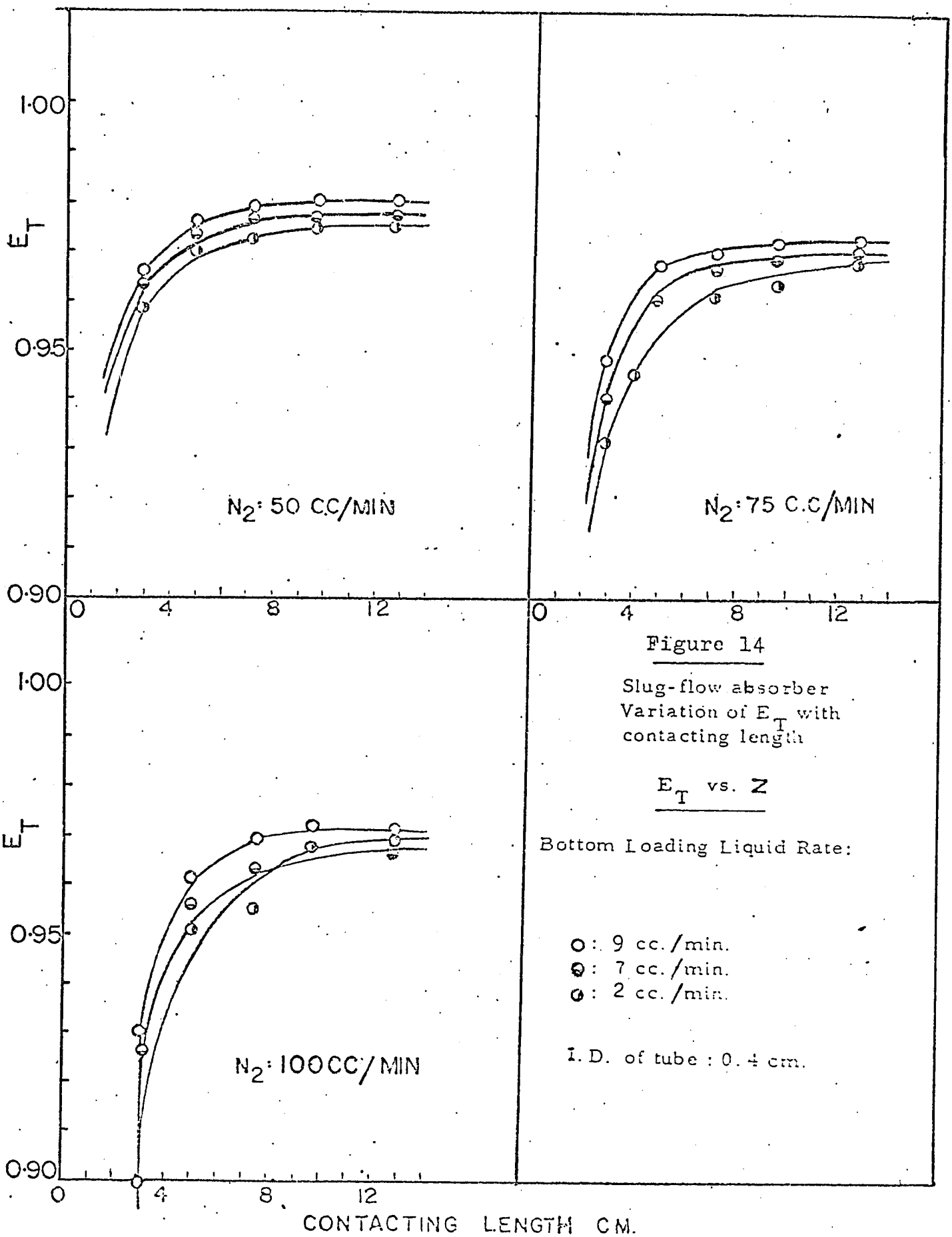

Figure 14

Slug-flow absorber
Variation of E_T with contacting length

E_T vs. Z

Bottom Loading Liquid Rate:

○ : 9 cc./min.
◐ : 7 cc./min.
◑ : 2 cc./min.

I. D. of tube : 0.4 cm.

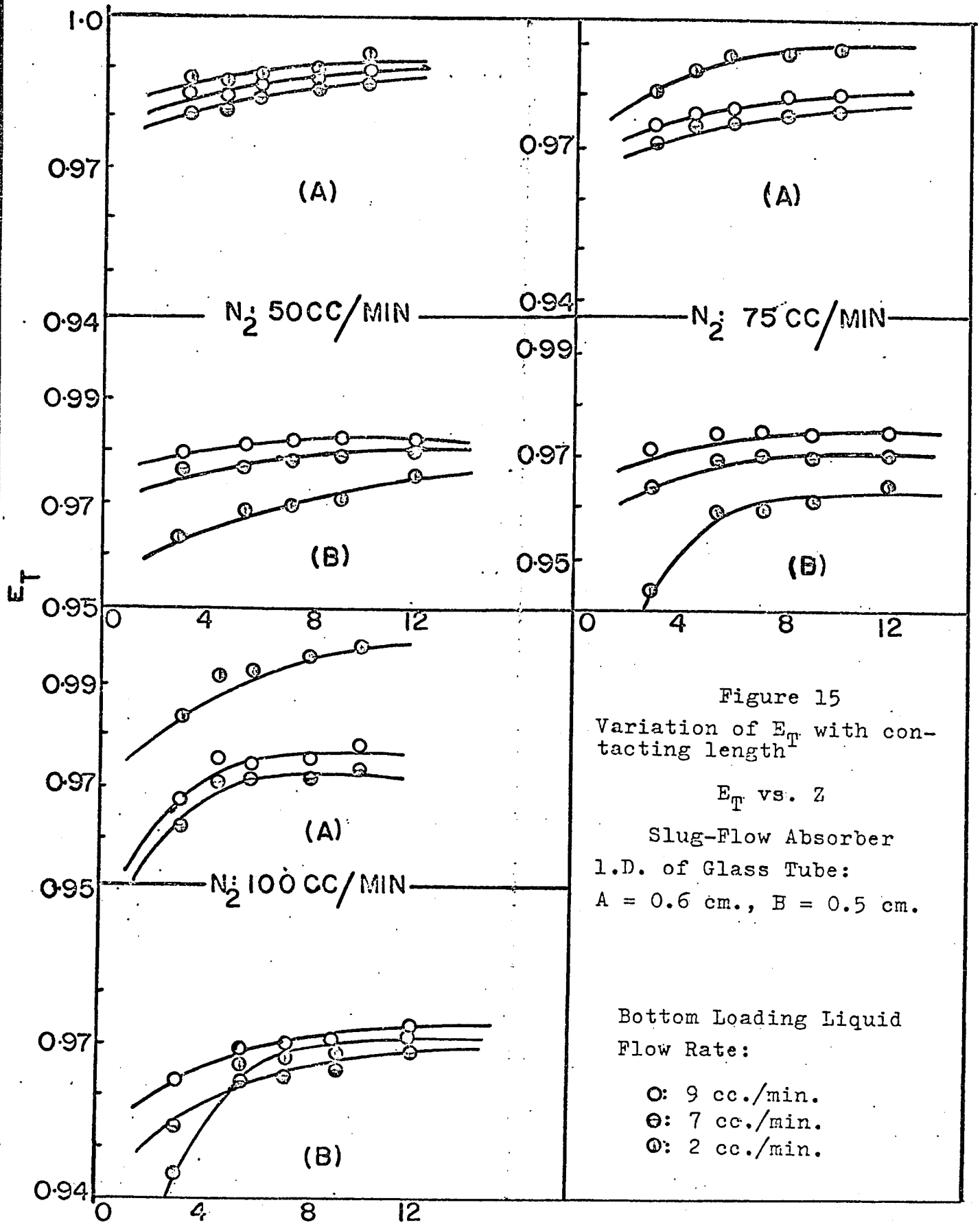

Figure 15

Variation of E_T with contacting length

E_T vs. Z

Slug-Flow Absorber

I.D. of Glass Tube:

A = 0.6 cm., B = 0.5 cm.

Bottom Loading Liquid Flow Rate:

O: 9 cc./min.
Θ: 7 cc./min.
①: 2 cc./min.

Efficiencies were also found to be an apparent function of liquid flow rate. The values of E_T were calculated on the basis of $y^* = 0$, which would hold at liquid rates of 7 and 9 cc. per min. if the liquid phase was completely mixed. In slug flow absorption, this assumption may not hold and an effect of liquid flow rate could be expected. This was observed by separation of the E_T versus contacting length curves for each liquid flow rate as shown in the Figures (14) and (15).

Incomplete mixing is considered to account for asymtopic values of E_T lower than 1.00 in these runs. For liquid flow rate equal to 2 cc. per min., y^* could not be taken as zero but the mixing of liquid appeared to be more complete as less entrainment was observed. In these runs, y^* was calculated with the assumption of a completely mixed liquid phase. For 0.6 cm. I.D. tube, all the E_T versus contacting length curves at this liquid rate (2 cc./min.) intersect or lie above the other curves at other liquid rate. This is assumed to be due to the more complete liquid mixing in the larger diameter tube.

Plots of $-\ln(1-E_T)$ against Θ for liquid rate at 7 cc. per min. are shown in Figure 16. Contact times were measured from visual observation and they are in the same order of magnitude as predicted by Davies (15). In the majority of these cases, the curves through these points were not straight lines. It can be seen that end-effect mass-transfer was high and the E_E values were of the order of magnitude of 0.94 to 0.98. At the liquid rate of 7 cc. per min. and lowest gas rate of 50 cc. per min., the plots give straight lines for 0.6 and 0.5 cm. columns and K_{OG} values were calculated from the slopes of the curves using equation (12) with surface areas and slug

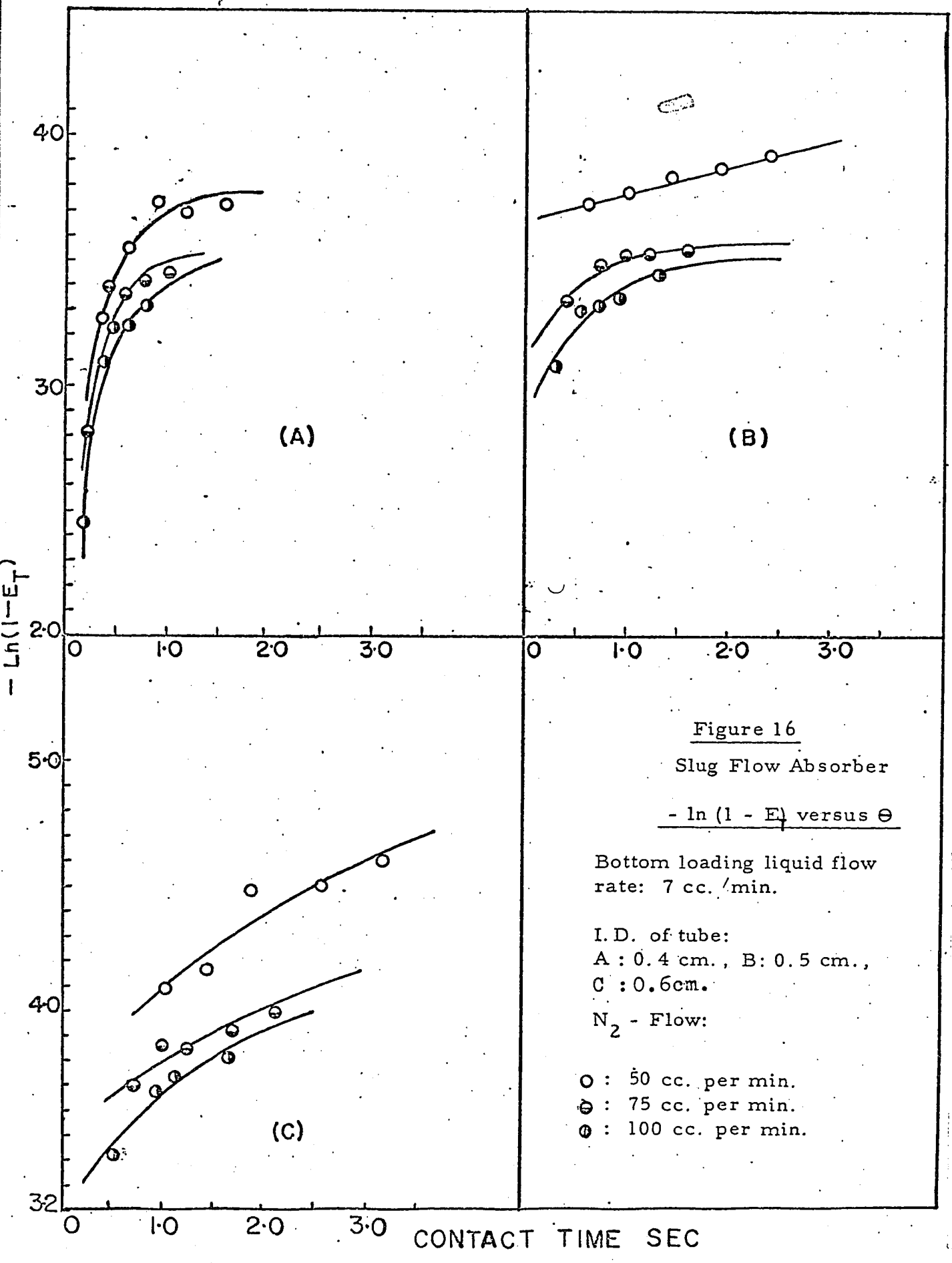

Figure 16

Slug Flow Absorber

- ln (1 - E) versus Θ

Bottom loading liquid flow rate: 7 cc./min.

I.D. of tube:
A : 0.4 cm., B: 0.5 cm.,
C : 0.6cm.

N_2 - Flow:

○ : 50 cc. per min.
◑ : 75 cc. per min.
● : 100 cc. per min.

frequency calculated from the photographic studies. The values of K_{OG} were found to be 0.029×10^{-4} and 0.025×10^{-4} g-mole/sec. atm. $cm.^2$ respectively. These values are in an order of magnitude lower than the values found for the bubble column and the wetted wall column. It is not sure at present whether this was a true reduction in K_{OG} or just simply the effect of incomplete liquid mixing, further work is required.

(II) Top Loading

In order to study the effect of liquid distribution, runs were carried with dodecane introduced at the top of the absorber and the results obtained are shown in Figure 17 and 18. E_T were slightly lower than those found for bottom loading absorber but were always high and the same general tendencies found; E_T decreased as the gas flow rate was increased but increased as tube diameter increased. The effect of liquid flow rate was again observed and asymtopic values less than 1.0 were found. Plots of $-\ln (1-E_T)$ versus contact time were made and curvature was again pronounced. End effects were high. No attempt made to evaluate overall-mass-transfer coefficients.

(e) Photographic Studies

Photographs were taken for the rising slugs as shown in Figure 19-A,B.C. For 0.4 and 0.5 cm. tubes, only those at gas rate of 50 cc. per min. were obtained because at the higher gas rates, slugs rose so fast that it was difficult for them to be pictured with an ordinary camera. The size and shape of slugs depend on tube diameter and liquid rates. As tube diameter was increased at constant liquid and gas flow rates, the gas slug shape changed and slug length decreased until hemispherical slugs were formed for tube diameter equal to 0.6 cm.

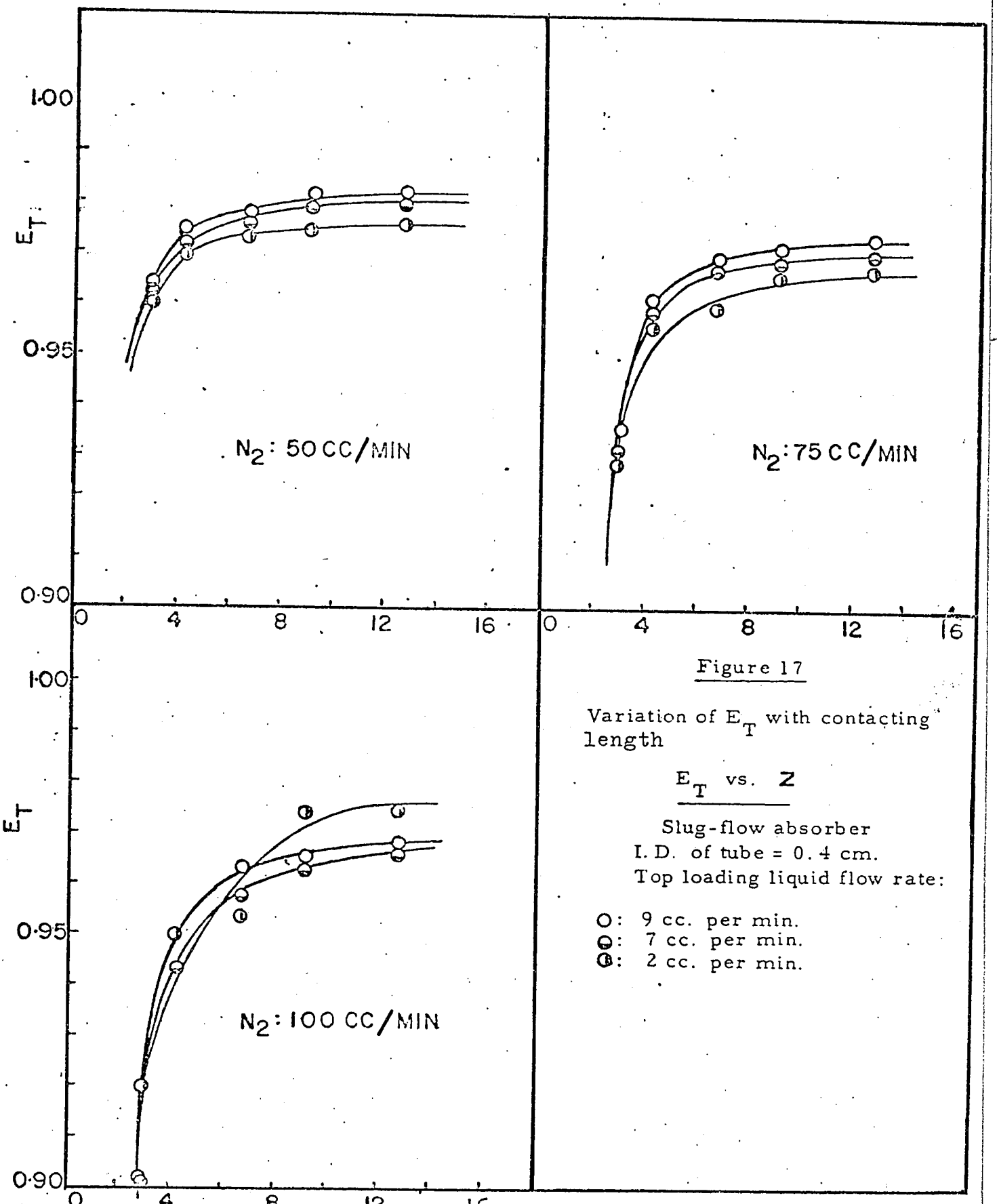

Figure 17

Variation of E_T with contacting length

E_T vs. Z

Slug-flow absorber
I. D. of tube = 0.4 cm.
Top loading liquid flow rate:

O: 9 cc. per min.
Q: 7 cc. per min.
1: 2 cc. per min.

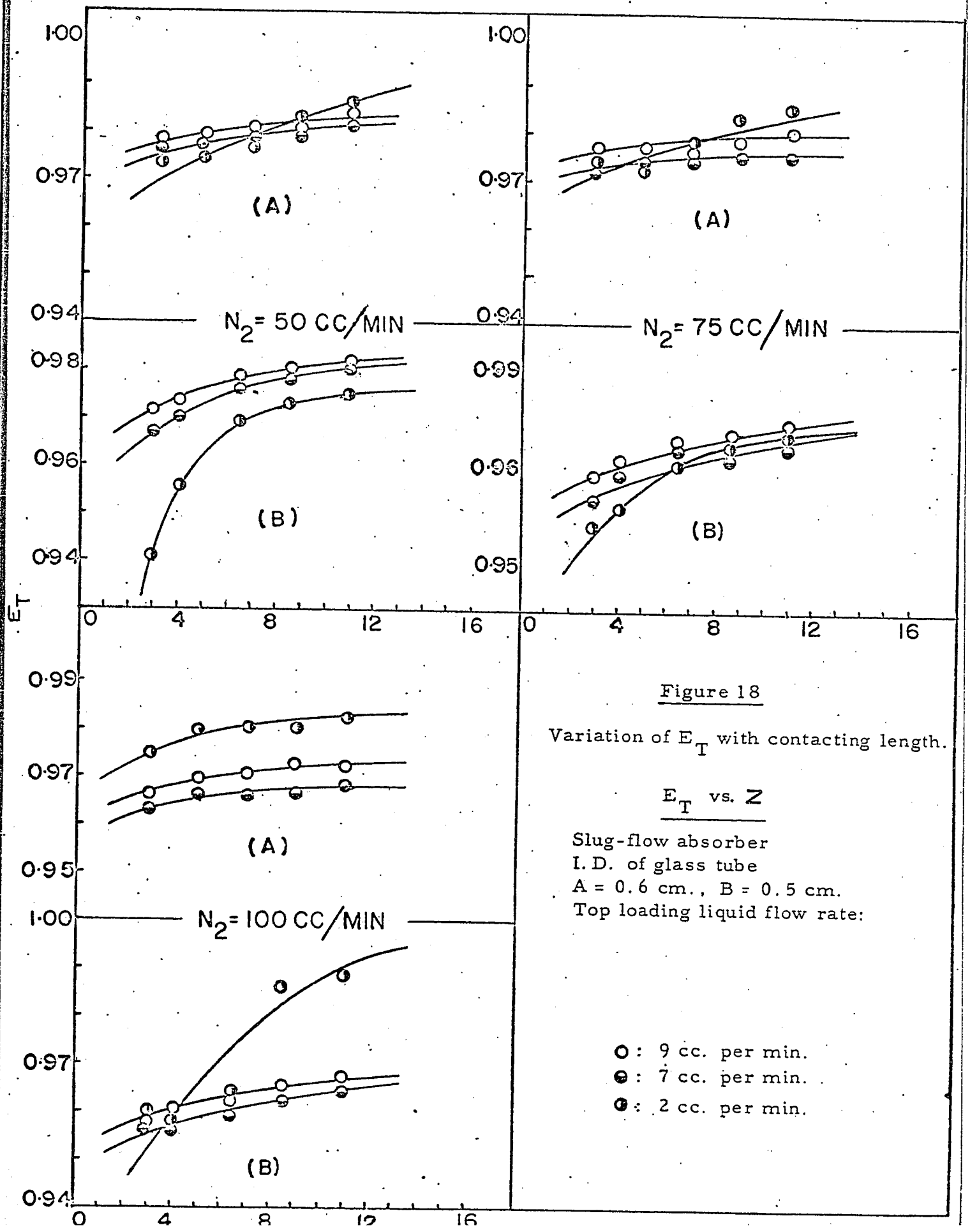

Figure 18

Variation of E_T with contacting length.

E_T vs. Z

Slug-flow absorber
I. D. of glass tube
A = 0.6 cm., B = 0.5 cm.
Top loading liquid flow rate:

○ : 9 cc. per min.
◒ : 7 cc. per min.
◐ : 2 cc. per min.

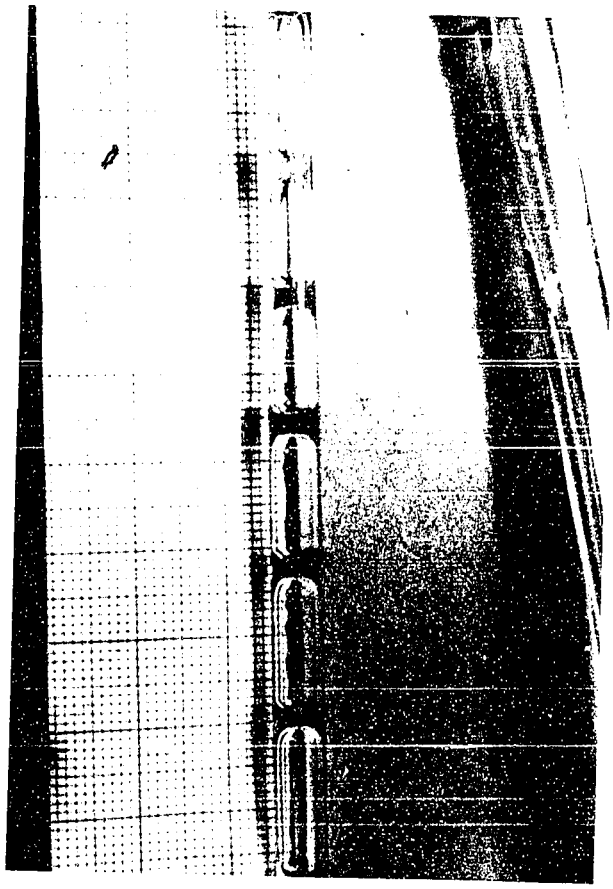

No. 1

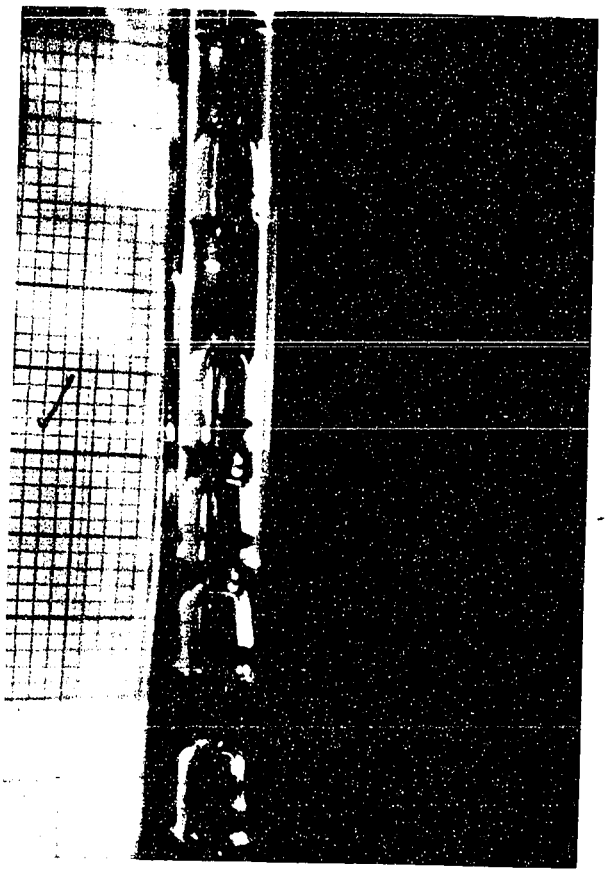

No. 2

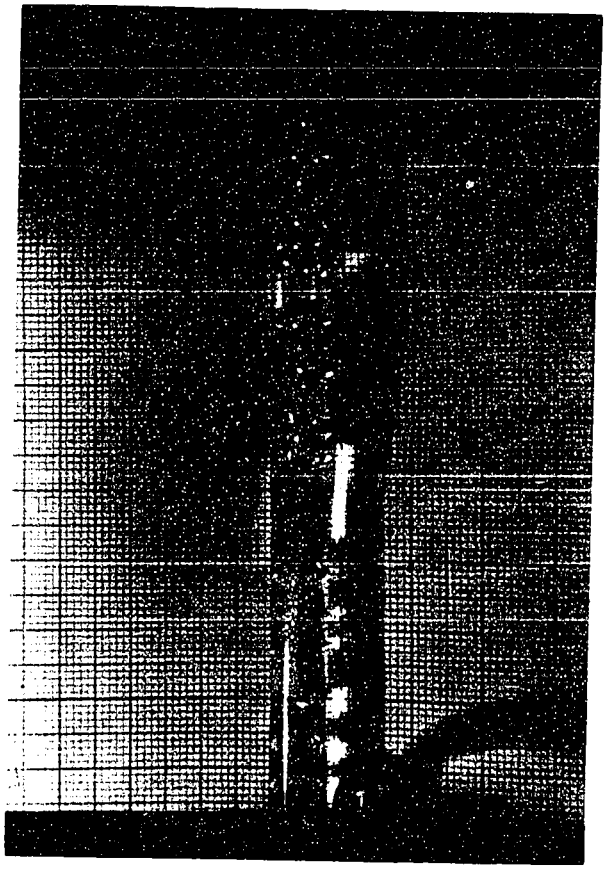

No. 3

Figure 19-A

Slug-flow absorber
Bottom loading liquid flow
Rate = 7 cc. per min.
N_2 Flow rate: 50 cc./min
I. D. of tube:

No. 1: 0.4 cm.
No. 2: 0.5 cm.
No. 3: 0.6 cm.

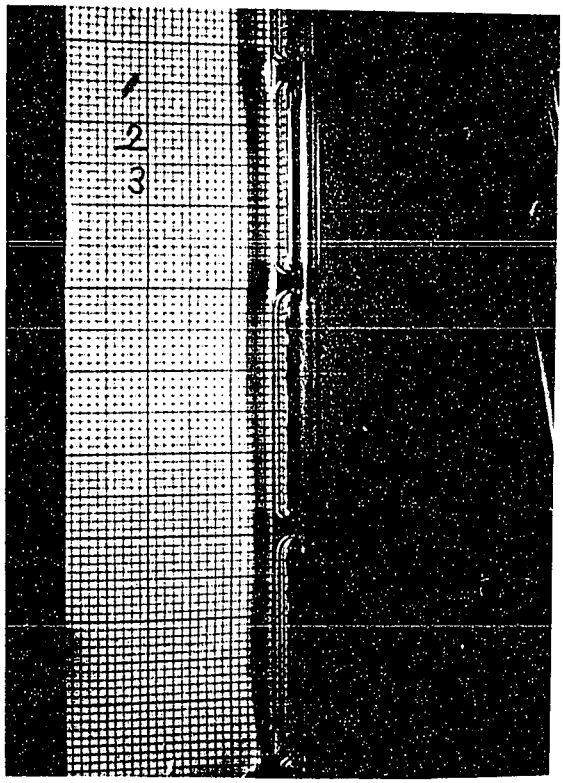

No. 1

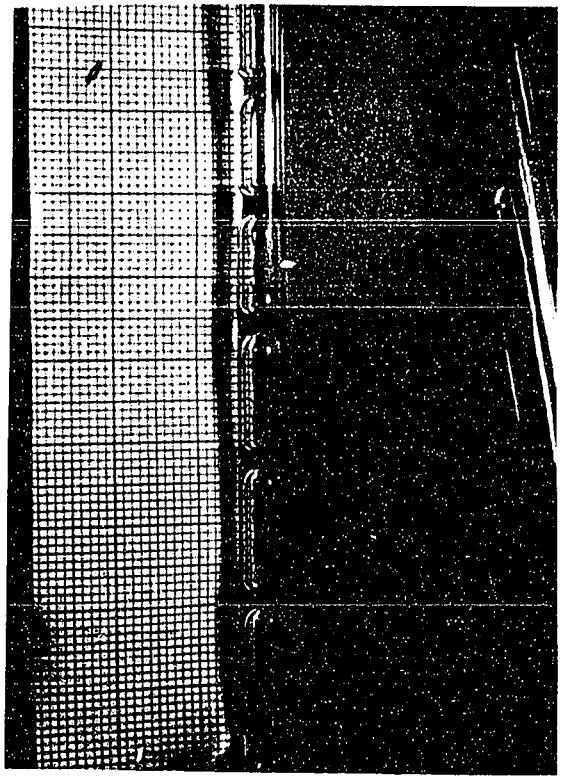

No. 2

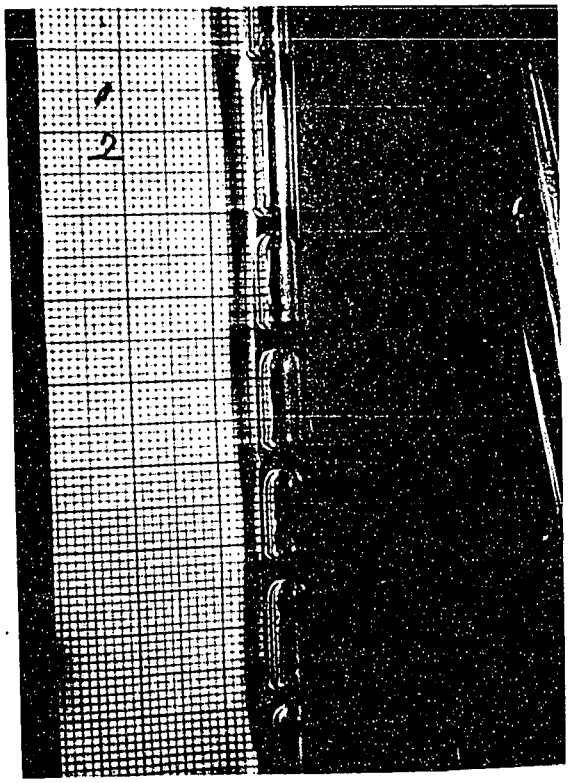

No. 3

Figure 19-B

Slug-flow absorber
N_2 - Flow rate: 50 cc./min
I.D. of tube: 0.4 cm.

Bottom loading liquid flow rate:

No. 1: 2 cc./min.
No. 2: 7 cc./min.
No. 3: 9 cc./min.

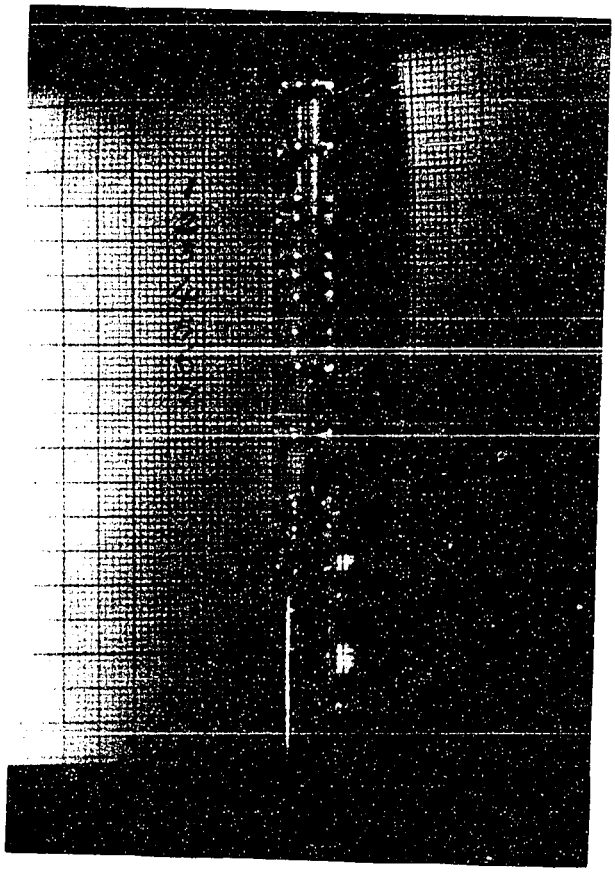

No. 1

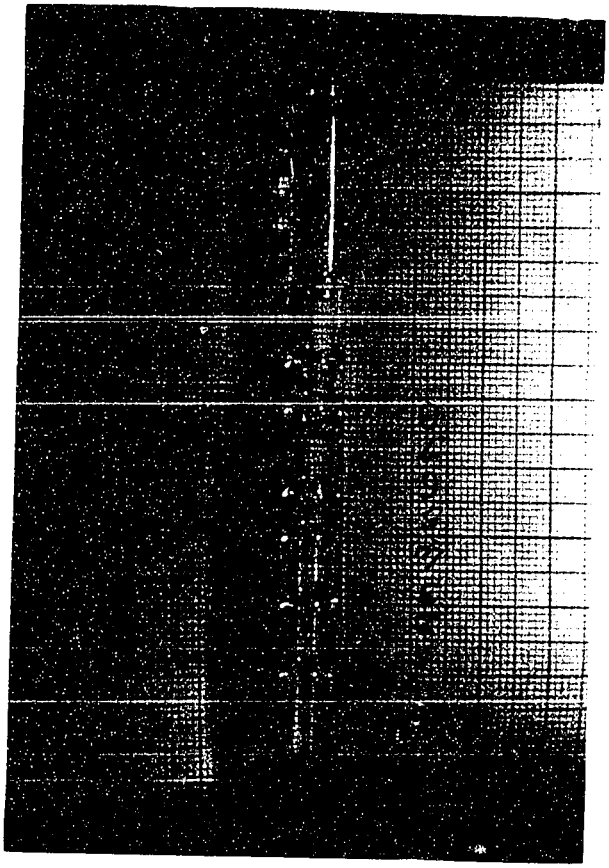

No. 2

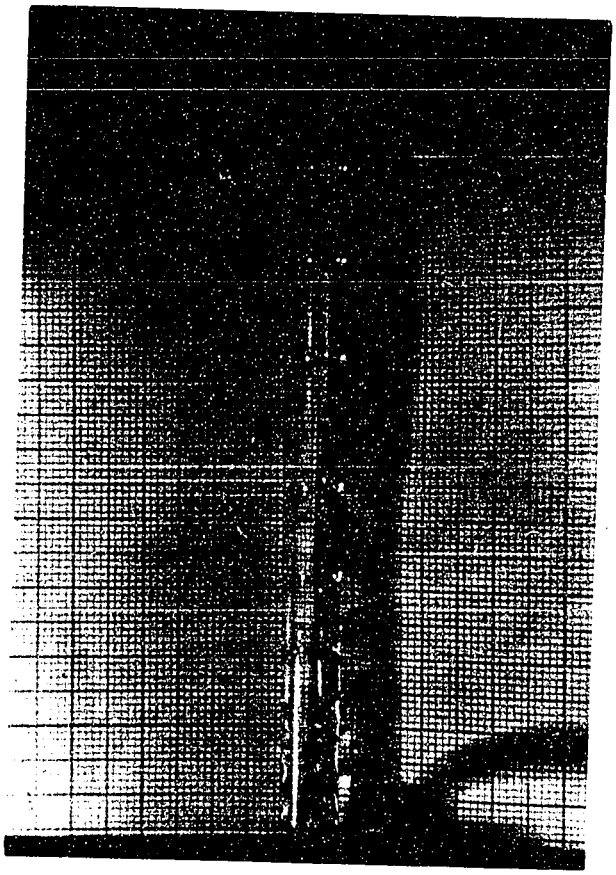

Figure 19-C

Slug-Flow Absorber
Bottom loading liquid flow rate:
2 cc./min.
I. D. of tube = 0. 6 cm.

N_2-Flow Rate:

No. 1: 50 cc. per min.
No. 2: 75 cc. per min.
No. 3: 100 cc. per min.

The slug length increased as the gas rate was increased but the opposite effect was observed when liquid rate was increased.

These studies showed that slug size could be controlled by varying gas and liquid flow rates until gas slugs were separated by thin film. Under these conditions, the mass-transfer taking place might represent those taking place in a foam.

V COMPARISON

E_T versus Θ plots at the same liquid and gas flow rate 7 and 50 cc. per min. respectively, for three different contacting methods are shown in Figure 20. The highest mass-transfer rate took place in the bubble column due to turbulent contacting conditions and are the function of the contacting apparatus. When the K_{OG} values for the bubble column and wetted wall column are compared, 0.35×10^{-4} to 0.15×10^{-4} (g-mole)/(sec.)(atm.)(cm.^{2}), the values for bubble column seem to be low for the E_T values found, as this could mean exceptionally high rates of end-effect mass-transfer. With the slug flow absorber, due to the large end-effect, the E_T values at low contact times were higher than those observed with the wetted wall column but as contact times increased E_T values for the slug-absorber fell below those for wetted wall column. The K_{OG} value for slug-flow absorber was 0.029×10^{-4} g-mole/(sec.)(atm.)(cm.^{2}) and small when compared to 0.15×10^{-4} g-mole/(sec.)(atm.)(cm.^{2}) of the wetted wall column. This could be due to suppresion of turbulence or incomplete mixing of the liquid.

The high end-effects observed complicated analysis of the data and further studies are necessary to conform the results.

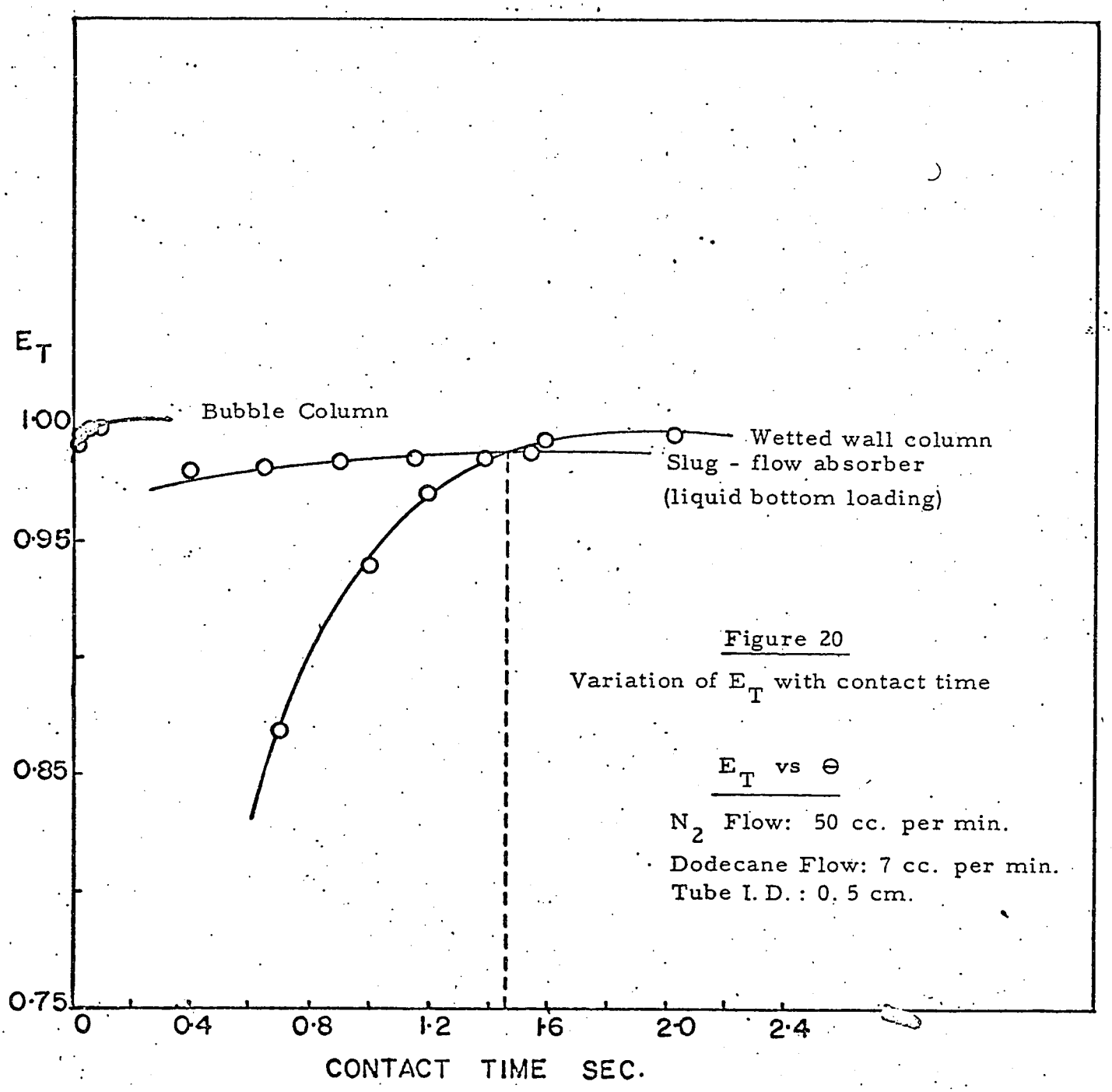

Figure 20

Variation of E_T with contact time

E_T vs Θ

N_2 Flow: 50 cc. per min.

Dodecane Flow: 7 cc. per min.

Tube I. D. : 0. 5 cm.

VII CONCLUSION

Mass-transfer has been studied under gas-phase controlled conditions for the system, nitrogen-hexane-dodecane, using three different methods of contacting. In all cases, high mass-transfer efficiencies were obtained. Mass-transfer rates were found to be dependent on contacting method, the highest overall mass-transfer rates being found in the bubble column where bubble rose freely through a liquid pool. Restriction of the bubble movement in slug-flow absorbers resulted in the lowest rise period mass-transfer rates. The high end-effect mass-transfer observed in bubble column and slug-flow absorber made it difficult to interpret the results and further work is required to eliminate or reduce the end effects so that these results can be confirmed.

Further, the photographic study of contacting in the slug flow absorber indicated that the gas liquid distribution was a function of both gas and liquid flow rates. Under certain conditions the gas slugs rose through the absorber, separated from each other by thin film of liquid. Under this condition, contacting might be more representative of the conditions existing on a plate column.

VIII RECOMMENDATION

The results of this study have indicated that mass-transfer rates may be reduced for gas-phase controlled absorption if slug flow is taking place. This reduction was accounted for by either restriction of bubble movement or incomplete liquid mixing. Further studies should be undertaken to confirm this finding.

In these studies, high end effect mass-transfer were observed and future investigation will be valueless if these end effects are

not reduced so that a significant amount of mass-transfer takes place in the rise period. Further studies should be undertaken to eliminate or reduce this end-effect mass-transfer.

REFERENCES

1. "Absorption and Extraction" Sherwood and Pigford, Mc-Graw Hill Book Company.

2. A. I. Ch. E., Research Committee final report, Tray Efficiencies in Distillation Column., Univ. of Delaware (1958).

3. A. I. Ch. E., Research Committee final report, Tray Efficiencies in Distillation Column, Univ. of Michigan (1959).

4. Barnet, W. I., and T. K. Sherwood, Ind. Eng. Chem. 33, 436 (1941).

5. Boelter, L. M. K., Trans. Am. Inst. Chem. Engrs, 39, 557 (1943).

6. Calderbank, P. H., Chem. Eng. Sci., 22, 209 (1967).

7. Calderbank, P. H., Trans. Instn. Chem. Engrs., 34, 79 (1956).

8. Calderbank, P. H., and A. C. Lochiel, Chem. Eng. Sci., 19, 485 (1964).

9. Chilton, T. H., and A. P. Colburn , Ind. Eng. Chem., 26, 1183 (1934).

10. Dal, V. I., and M. A. Vitkina, J. Chem. Ind., 10, 609 (1949).

11. Drew, T. B., Trans. Am. Inst. Chem. Engrs., 26, 26 (1931).

12. Drew, Hougen and McAdams, Ind. Eng. Chem. 23, 936 (1931).

13. Datta, R. L., D. H. Napier and D. M. Newitt, Trans. Inst. Chem. Eng., 14, 28 (1950).

14. Deindorfer, F. H., Humphrey, A. E., Ind. Eng. Chem., 53, 755 (1961).

15. Davies, R. M., and Taylor, G. I., Proc. R. Soc., 200A, 375 (1950).

16. E. Ruckenstein, Chem. Eng. Sci., 19, 505 (1964).

17. Furter, W.F., Can. J. of Chem. Eng. 42-43, 349 (1964-65).

18. Friedman, S. J., and C.O. Miller, Ind. Eng. Chem., 33, 885 (1941).

19. Gilliland, E. R., and T.K. Sherwood, Ind. Eng. Chem., 26, 516 (1934).

20. Groothuis, H., and Kramers, H. Chem. Eng. Sci., 1, 17 (1955).

21. Garner, F.H., and Hammerton, Chem. Eng. Sci., 3, 1 (1954).

22. Golding, J.A., Graydon, W.F., and Johnson, A.I., Trans. Inst. Chem. Engrs., 46, 172 (1968).

23. Gianetto, A., Chem. et. Ind., 42, 1100 (1960).

24. Hollings, H., and L. Silver., Trans. Inst. Chem. Engrs., 12, 49 (1934).

25. Halberstadt and Prausnitz, Z. Angrew Chim., 43, 970 (1920), as reported by (13).

26. Hamielec, A.E., M.A.Sc. Thesis, U. of Toronto (1958).

27. Haslam, R.T., Herthey, R.L., and Keen, R.H., Ind. Eng. Chem., 16, 1224 (1924).

28. Haselden, G.G., and Thorogood, R.M. Trans. Instn. Chem. Engrs., 42, 781 (1964).

29. Johnson, A.I., and J.M. Hay, A.I.Ch.E., 6, 373 (1960).

30. Johnson, A.I., Hamielec, A.E., Ward, D., and Golding, J.A., Can. J. Chem. Eng., 36, 221 (1958).

31. Krebs, R.W., Ph.D. thesis, Univ. of Illinois (1938).

32. "Mass transfer and Absorber", Hobler, Pergamm Press, (1966).

33. Poutanen, A.A., Ph.D. thesis in Chem. Eng., Univ. of Toronto (1960).

34. Schnurman, Z.F., Phy. Chim., 143, 456-74, 5-6 (1929), as reported by (13).

35. Timson, W. J., and Dunn, C. E., Ind. Eng. Chem. 52, 799 (1960).

36. Uchida, Shun-Chi and Thigerus Maeda, J. Soc. Chem. Ind. Japan, Supply, Binding, 38, 625 (1935). as reported by (33).

37. Yauo, To., and Kawai Ko., J. Soc. Chem. Engrs., Japan, 21, 413 (1957). as reported by (33).

38. Zwiderweg, F. J., and A. Harmens, Chem. Eng. Sci., 9, 89 (1958).

NOMENCLATURE

A	:	Surface area, $cm.^2$
A_S	:	Surface area of slugs, $cm.^2$
D_V	:	Molecular diffusivity, cm./sec.
E_C	:	Coalescence mass-transfer efficiency
E_S	:	Rise period mass-transfer efficiency
E_E	:	Combined end-effect mass-transfer
E_F	:	Formation mass-transfer efficiency
E_T	:	Overall mass-transfer efficiency
G	:	Molal gas flow rate, g-mole/sec.
K_{OG}	:	Overall gas phase mass-transfer coefficient, g-mole/$(cm)^2$ (sec)(atm).
L	:	Liquid flow rate, cc./min.
M.V.	:	Millivolt
N	:	Length of wetted wall, cm.
N_{Re}	:	Reynold number
P	:	Total pressure, atm.
V	:	Velocity, cm./sec.
$\overline{V}$	:	Volume of bubbles $cm.^3$
W	:	Mass flow rate g/sec.
X	:	Hexane mole fraction in liquid phase
Z	:	Contacting length, cm.
d	:	Bubble diameter, cm.
f	:	Frequency, bubbles/sec.
f_s	:	Frequency, slugs/sec.
g	:	Acceleration constant, $cm./sec.^2$
m.a	:	Milliampere
r	:	Radius, cm.
y	:	Mole fraction of hexane in the gas phase
y^*	:	Mole fraction of hexane that would be in equilibrium with the liquid phase
η_ℓ	:	Liquid viscosity, g-/cm.-sec.
σ	:	Surface tension, g-force/cm.-sec.
Θ	:	Contact time, sec.
ρ	:	Gas density, g/cc.

APPENDICES

APPENDIX 1

TABULATED EXPERIMENTAL DATA

NOMENCLATURE

A - Wetted wall column

B - Bubble column

C - Slug flow absorber

SUBSCRIPT

1 - refers to liquid flow rate of 2 cc. per min.

2 - refers to liquid flow rate of 7 cc. per min.

3 - refers to liquid flow rate of 9 cc. per min.

i.e. A_2-3 refers to a run carried out with the wetted wall column at a liquid rate of 7 cc. per min.

TABLE 1-1

etted Wall Column I.D. = 0.4 cm.
ifective Cross Section Area = 0.366 cm^2
trogen Flow Rate = 50 c.c. per min.

ın).	1 Contacting Length cm.	2 Saturator Pressure mm. Hg	3 Millivolt Reading M.V.	4 y_{off} mole fraction x 10^2	5 y_{on} mole fraction x 10^2	6 E_T	7 -ln (1-E_T)	8 Contact Time, Θ sec.
-1	9.8	764	0.06	0.012	4.587	0.9973	7.958	1.205
-1	9.8	764	0.045	0.009	4.587	0.9980	8.518	1.205
-2	7.8	764	0.145	0.029	4.563	0.9936	6.215	0.959
-2	7.8	764	0.15	0.030	4.563	0.9934	5.941	0.959
-3	6.6	770	0.245	0.049	4.547	0.9892	5.427	0.812
-3	6.6	770	0.25	0.05	4.547	0.9890	5.524	0.812
-4	5.8	769	0.475	0.08	4.551	0.9824	4.041	0.713
-4	5.8	769	0.43	0.072	4.551	0.9841	4.142	0.713
-5	5	768	0.73	0.146	4.556	0.9679	3.439	0.615
-5	5	768	0.73	0.146	4.556	0.9679	3.439	0.615
-6	3.2	766	2.20	0.442	4.569	0.9033	2.339	0.394
-6	3.2	766	2.175	0.437	4.569	0.9042	2.346	0.394
-7	9.8	764	0.05	0.010	4.587	0.9978	8.080	
-7	9.8	764	0.05	0.010	4.587	0.9978	8.113	
-8	7.8	764	0.15	0.030	4.563	0.9934	5.941	
-8	7.8	764	0.15	0.030	4.563	0.9927	5.976	
-9	6.6	770	0.26	0.052	4.547	0.9886	5.533	
-9	6.6	770	0.28	0.051	4.547	0.9876	5.651	
-10	5.8	769	0.45	0.075	4.551	0.9834	4.10	
-10	5.8	769	0.47	0.079	4.551	0.9826	4.052	

Run No.	1	2	3	4	5	6	7	8
A_2-11	5	768	0.84	0.168	4.556	0.9632	3.302	
-11	5	768	0.80	0.16	4.556	0.9653	3.359	
-12	3.2	766	2.23	0.448	4.569	0.9019	2.3221	
-12	3.2	766	2.20	0.442	4.569	0.9026	2.329	
Nitrogen Flow Rate = 75 cc per min.								
A_2-13	9.8	769	0.18	0.036	4.557	0.9921	4.9340	0.803
-13	9.8	769	0.20	0.040	4.557	0.9921	4.9346	0.803
-14	7.8	769	0.64	0.128	4.525	0.9719	3.5726	0.639
-14	7.8	769	0.65	0.126	4.525	0.9715	3.5585	0.639
-15	6.6	773	1.03	0.206	4.528	0.9545	3.091	0.541
-15	6.6	773	0.91	0.182	4.528	0.9596	3.209	0.541
A_2-16	5.8	770	1.275	0.255	4.544	0.9438	2.879	0.476
-16	5.8	770	1.26	0.251	4.544	0.9448	2.897	0.476
-17	5	772	1.845	0.369	4.535	0.9186	2.508	0.410
-17	5	772	1.82	0.362	4.535	0.9202	2.53	0.410
-18	3.2	770	4.06	0.8223	4.545	0.8191	1.709	0.262
-18	3.2	770	4.07	0.8223	4.545	0.819	1.175	0.262
A_3-19	9.8	769	0.18	0.036	4.557	0.9921	4.8418	
-19	9.8	769	0.20	0.040	4.557	0.9922	4.8567	
-20	7.8	769	0.63	0.126	4.525	0.9724	3.5906	
-20	7.8	769	0.63	0.126	4.525	0.9724	3.5899	
-21	6.6	773	0.95	0.19	4.528	0.9580	3.1707	
-21	6.6	773	1.01	0.202	4.528	0.9554	3.11	
-22	5.8	770	1.335	0.267	4.544	0.9413	2.835	
-22	5.8	770	1.29	0.258	4.544	0.9432	2.869	
-23	5	772	2.1	0.421	4.535	0.907	2.375	

Run No.	1	2	3	4	5	6	7	8
2-23	5	772	1.86	0.371	4.535	0.9182	2.504	
-24	3.2	770	4.23	0.8572	4.545	0.8114	1.709	
-24	3.2	770	4.15	0.8402	4.545	0.8151	1.6876	
2 Flow Rate = 100 cc. per min.								
2-25	9.8	773	0.52	0.1	4.579	0.9770	3.773	0.603
-25	9.8	773	0.53	0.106	4.579	0.9766	3.7557	0.603
-26	7.8	773	1.49	0.299	4.547	0.9339	2.717	0.48
-26	7.8	773	1.493	0.2995	4.525	0.9339	2.717	0.480
-27	6.6	777	1.98	0.396	4.504	0.9120	2.431	0.406
-27	6.6	777	1.975	0.379	4.504	0.9158	2.4750	0.406
-28	5.8	773	2.3	0.463	4.528	0.8979	2.281	0.357
-28	5.8	773	2.45	0.4945	4.528	0.8907	2.214	0.357
-29	5	776	3.05	0.62	4.51	0.8652	2.004	0.308
-29	5	776	3.09	0.628	4.51	0.861	1.9723	0.308
-30	3.2	774	5.785	1.21	4.522	0.7324	1.3186	0.197
-30	3.2	774	5.822	1.22	4.522	0.7306	1.3111	0.197
3-31	9.8	773	0.57	0.114	4.579	0.9748	3.6816	
-31	9.8	773	0.51	0.102	4.579	0.9775	3.7931	
-32	7.8	773	1.53	0.306	4.547	0.9323	2.693	
-32	7.8	773	1.51	0.301	4.525	0.9335	2.711	
-33	6.6	777	1.975	0.395	4.504	0.9123	2.4342	
-33	6.6	777	1.94	0.388	4.504	0.9140	2.452	
-34	5.8	777	2.309	0.465	4.528	0.8973	2.276	
-34	5.8	777	2.40	0.483	4.528	0.8933	2.234	
-35	5	776	3.13	0.636	4.51	0.8586	1.9566	
-35	5	776	3.21	0.651	4.51	0.8556	1.9359	

Run No.	1	2	3	4	5	6	7	8
3-36	3.2	774	5.982	1.252	4.522	0.7231	1.2839	
-36	3.2	774	5.91	1.24	4.522	0.7266	1.297	

TABLE 1-2

Wetted Wall Column I.D. = 0.5 cm.
Effective Cross-Section Area = 0.4679 $cm.^2$
Nitrogen Flow Rate = 50 cc. per min.

Run No.	1	2	3	4	5	6	7	8
2-37	10.1	763	0.055	0.011	4.587	0.9976	6.0334	2.036
-37	10.1	763	0.055	0.011	4.587	0.9976	6.0334	2.036
-38	7.9	767	0.155	0.031	4.556	0.9932	4.9917	1.593
-38	7.9	767	0.15	0.030	4.556	0.9934	5.022	1.593
-39	6.9	766	0.325	0.065	4.571	0.9858	4.2552	1.391
-39	6.9	766	0.345	0.069	4.571	0.9849	4.1937	1.391
-40	6	766	0.63	0.126	4.566	0.9724	2.43	1.210
-40	6	766	0.586	0.117	4.566	0.9744	3.527	1.210
-41	5	768	1.08	0.216	4.559	0.9526	1.924	1.01
-41	5	768	1.0	0.20	4.559	0.9561	2.961	1.01
-42	3.5	766	2.87	0.582	4.567	0.8725	2.06	0.706
-42	3.5	766	2.95	0.5995	4.567	0.8687	2.033	0.706
3-43	10.1	763	0.06	0.012	4.587	0.9970	6.1	
-43	10.1	763	0.0522	0.0104	4.587	0.9977	6.076	
-44	7.9	767	0.15	0.030	4.556	0.9934	5.022	
-44	7.9	767	0.16	0.032	4.556	0.9930	4.963	

Run No.	1	2	3	4	5	6	7	8
A_3-45	6.9	766	0.315	0.063	4.571	0.9862	4.2838	
-45	6.9	766	0.35	0.070	4.571	0.9847	4.1806	
-46	6	766	0.67	0.134	4.566	0.9706	3.591	
-46	6	766	0.63	0.126	4.566	0.9724	3.660	
-47	5	768	1.255	0.251	4.559	0.9449	3.049	
-47	5	768	1.17	0.234	4.559	0.9486	3.126	
-48	3.5	766	3.120	0.634	4.567	0.8612	1.9981	
-48	3.5	766	3.05	0.61	4.567	0.8664	1.991	
N_2 Flow Rate = 75 cc. per min.								
A_2-49	10.1	769	0.225	0.045	4.550	0.9901	4.6161	1.358
-49	10.1	769	0.228	0.045	4.550	0.9901	4.6161	1.358
-50	7.9	771	0.55	0.11	4.539	0.9757	3.718	1.062
-50	7.9	771	0.64	0.128	4.539	0.9718	3.5692	1.062
-51	6.9	768	1.13	0.226	4.557	0.9504	3.0042	0.928
-51	6.9	768	1.08	0.216	4.557	0.9526	3.049	0.928
-52	6	770	1.9	0.38	4.542	0.9163	2.5906	0.808
-52	6	770	2.01	0.40	4.542	0.9119	2.432	0.808
-53	5	778	2.22	0.462	4.536	0.8981	2.968	0.672
-53	5	778	2.275	0.457	4.536	0.8993	2.2569	0.672
-54	3.5	770	4.76	0.966	4.543	0.7874	1.5601	0.471
-54	3.5	770	4.80q	0.974	4.543	0.7856	1.5402	0.471
A_3-55	10.1	769	0.228	0.045	4.550	0.9901	4.6161	
-55	10.1	769	0.230	0.046	4.550	0.9900	4.600	
-56	7.9	771	0.575	0.114	4.539	0.9748	3.6815	
-56	7.9	771	0.62	0.124	4.539	0.9727	3.6014	
-57	6.9	768	1.1	0.22	4.557	0.9517	3.0104	
-57	6.9	768	1.15	0.23	4.557	0.9495	2.986	
-58	6	770	1.99	0.399	4.542	0.9121	2.48	

un o.	1	2	3	4	5	6	7	8
3 -58	6	770	2.15	0.430	4.542	0.9049	2.429	
-59	5	773	2.36	0.462	4.536	0.8981	2.284	
-59	5	773	2.405	0.457	4.542	0.8932	2.237	
-60	3.5	770	4.81	0.9755	4.543	0.7852	1.5384	
-60	3.5	770	4.84	0.982	4.543	0.7839	1.5321	
2 Flow Rate = 100 cc. per min.								
2 -61	10.1	775	0.56	0.112	4.527	0.9753	3.7016	1.018
-61	10.1	773	0.579	0.114	4.527	0.9746	3.6698	1.018
-62	7.9	775.6	1.27	0.254	4.516	0.9438	2.894	0.796
-62	7.9	776.0	1.30	0.26	4.516	0.9442	2.8688	0.796
-63	6.9	772	1.985	0.397	4.530	0.9123	2.986	0.696
-63	6.9	772	2.09	0.4189	4.530	0.9075	2.457	0.696
-64	6	774	3.115	0.633	4.519	0.8599	2.354	0.610
-64	6	774	3.21	0.652	4.519	0.8557	1.906	0.610
-65	5	766	3.71	0.751	4.519	0.8338	1.7949	0.504
-65	5	766	3.70	0.75	4.519	0.8340	1.7961	0.504
-66	3.5	774	6.26	1.352	4.519	0.7068	1.223	0.353
-66	3.5	774	6.40	1.38	4.519	0.6946	1.1805	0.353
3 -67	10.1	773	0.57	0.115	4.527	0.9748	3.6737	
-67	10.1	773	0.57	0.114	4.527	0.9748	3.6698	
-68	7.9	775	1.27	0.254	4.516	0.9438	2.8794	
-68	7.9	776	1.26	0.26	4.516	0.9442	2.8688	
-69	6.9	772	1.97	0.394	4.530	0.9130	2.457	
-69	6.9	772	1.99	0.399	4.530	0.9119	2.381	
-70	6	774	3.133	0.637	4.519	0.8513	1.966	
-70	6	774	3.25	0.66	4.519	0.8539	1.936	

Run No.	1	2	3	4	5	6	7	8
A_3-71	5	776	3.85	0.78	4.519	0.8274	1.7572	
-71	5	776	3.80	0.774	4.519	0.8287	1.7648	
-72	3.5	774	6.44	1.388	4.519	0.6928	1.1805	
-72	3.5	774	6.50	1.40	4.519	0.6902	1.1745	

TABLE 1-3

Rising Bubble Column
Nitrogen Flow Rate = 50 cc. per min.
Capillary I.D. = 0.1 cm.

Run No.	1	2	3	4	5	6	7	8
B_2-1	1	766	0.148	0.03	4.56	0.9935	5.059	0.049
-1	1	766	0.154	0.031	4.56	0.9933	5.006	0.049
-2	1.5	766	0.07	1.014	4.56	0.9969	5.776	0.087
-2	1.5	766	0.07	0.014	4.56	0.9969	5.776	0.087
-3	2.0	763	0.05	0.010	4.54	0.9979	6.168	0.125
-3	2.0	763	0.035	0.007	4.54	0.9985	6.504	0.125
-4	2.5	763	0.022	0.0044	4.54	0.9991	7.015	0.162
-4	2.5	763	0.02	0.004	4.54	0.9991	7.015	0.162
-5	3.0	763	0.02	0.004	4.54	0.9991	7.015	0.200
-5	3.0	763	0.02	0.004	4.54	0.9991	7.015	0.200

Nitrogen Flow Rate = 75 cc. per min.

Run No.	1	2	3	4	5	6	7	8
B_2-6	1	769	0.23	0.046	4.556	0.9899	4.5967	0.0410
-6	1	769	0.20	0.040	4.556	0.9912	4.735	0.0410
-7	1.5	769	0.13	0.026	4.556	0.9940	5.12	0.076
-7	1.5	769	0.15	0.030	4.556	0.9934	5.25	0.076
-8	2.0	766	0.07	0.014	4.57	0.9969	5.78	0.1110
-8	2.0	766	0.08	0.014	4.57	0.9965	5.66	0.1110
-9	2.5	766	0.05	0.010	4.57	0.9978	6.124	0.145
-9	2.5	766	0.03	0.006	4.57	0.9987	6.646	0.145
-10	3.0	766	0.02	0.004	4.57	0.9991	7.014	0.180
-10	3.0	766	0.03	0.006	4.57	0.9987	6.646	0.180

Nitrogen Flow Rate = 100 cc. per min.

B_2-11	1	773	0.35	0.07	4.536	0.9846	4.15	0.035
-11	1	773	0.33	0.06	4.536	0.9855	4.24	0.035
-12	1.5	773	0.22	0.044	4.536	0.9903	4.64	0.068
-12	1.5	773	0.20	0.040	4.536	0.9912	4.74	0.068
-13	2.0	770	0.14	0.028	4.54	0.9940	5.12	0.101
-13	2.0	770	0.15	0.030	4.54	0.9934	5.25	0.101
-14	2.5	770	0.10	0.020	4.54	0.9956	5.430	0.134
-14	2.5	770	0.08	0.016	4.54	0.9965	5.658	0.134
-15	3.0	770	0.05	0.010	4.54	0.9978	6.121	0.167
-15	3.0	770	0.05	0.010	4.54	0.9978	6.121	0.167

TABLE 1-4

I.D. of Slug Flow Absorber = 0.4 cm.
Nitrogen Flow Rate = 50 cc. per min.
Top Loading

Run No.	1	2	3	4	5	6	7	$y^* \times 10^2$
C_1-1	12.65	768	1.47	0.294	4.557	0.9757	3.268	0.187
-2	9.1	769	1.48	0.30	4.551	0.9738	3.20	0.1819
-3	6.75	769	1.53	0.306	4.553	0.9716	3.140	0.1819
-4	4.2	766	1.55	0.31	4.572	0.9705	3.167	0.1820
-5	3	766	1.76	0.352	4.573	0.960	2.862	0.1805
C_2-6	12.65	769	0.445	0.089	4.554	0.9804	3.467	
-7	9.1	769	0.47	0.094	4.551	0.9793	3.418	
-8	6.75	769	0.537	0.108	4.557	0.9740	3.301	
-9	4.2	766	0.643	0.133	4.572	0.9718	3.146	
-10	3	766	0.83	0.174	4.569	0.9625	2.896	
C_3-11	12.65	769	0.428	0.0855	4.554	0.981	3.907	
-12	9.1	770	0.438	0.0875	4.549	0.9807	3.481	
-13	6.75	769	0.495	0.097	4.553	0.9780	3.366	
-14	4.2	766	0.585	0.118	4.571	0.9744	3.229	
-15	3	766	0.82	0.164	4.569	0.9641	2.894	

Nitrogen Flow Rate = 75 cc. per min.

C_1-16	12.65	772	2.024	0.4047	4.534	0.9668	3.004	0.2637
-17	9.1	774	2.05	0.411	4.526	0.9653	2.96	0.2629
-18	6.75	773	2.18	0.437	4.530	0.9588	2.811	0.2615
-19	4.2	770	2.26	0.448	4.547	0.9557	2.746	0.2617
-20	3	763	2.78	0.556	4.527	0.9280	2.324	0.2628
C_2-21	12.65	772	0.67	0.1354	4.534	0.9705	3.106	

un o.	1	2	3	4	5	6	7	$y^* \times 10^2$
2-22	9.1	773	0.706	0.141	4.528	0.9688	3.059	
-23	6.75	773	0.74	0.148	4.530	0.9673	3.015	
-24	4.2	770	0.97	0.196	0.4548	0.9575	2.78	
-25	3	773	1.545	0.309	0.4525	0.9317	2.364	
3-26	12.65	772	0.59	0.119	0.4534	0.9741	3.218	
-27	9.1	774	0.65	0.130	0.4526	0.9714	3.132	
-28	6.75	773	0.693	0.1385	0.4530	0.9694	3.070	
-29	4.2	770	0.90	0.180	0.4571	0.9606	2.85	
-30	3	773	1.47	0.293	0.4526	0.9352	2.412	
itrogen Flow Rate = 100 cc. per min.								
1-31	12.65	776	2.55	0.451	4.510	0.9744	3.228	0.344
-32	9.1	777	2.26	0.452	4.52	0.9740	3.22	0.3437
-33	6.75	773	2.66	0.537	4.53	0.9694	3.07	0.3390
-34	3	777	3.34	0.677	4.503	0.920	2.233	0.920
-35	12.65	777	0.755	0.150	4.510	0.9665	3.000	
-36	9.1	777	0.82	0.164	4.505	0.9636	2.92	
-37	6.75	773	0.945	0.189	4.526	0.9583	2.801	
-38	3	777	2.20	0.440	4.503	0.9019	2.050	
3-39	12.67	777	0.725	0.145	4.510	0.9678	3.028	
-40	9.1	777	0.773	0.155	4.504	0.9655	2.965	
-41	6.75	777	0.843	0.168	4.526	0.9630	2.905	
-42	3	773	2.145	0.429	4.503	0.9047	2.073	

TABLE 1-5

I.D. of Slug Flow Absorber = 0.5 cm.
Nitrogen Flow Rate = 50 cc. per min.
Top Loading

Run No.	1	2	3	4	5	6	7	$y^* \times 10^2$
C_1-43	11	762	1.47	0.294	4.593	0.9750	3.68	0.1837
-44	8.6	762	1.50	0.30	4.593	0.9733	3.51	0.1835
-45	6.5	763	1.59	0.318	4.588	0.9693	3.48	0.1829
-46	4.1	765	1.818	0.364	4.575	0.9564	3.13	0.1815
-47	3	760	2.175	0.435	4.607	0.9421	2.850	0.1786
C_2-48	11	761	0.45	0.090	4.598	0.9804	3.931	
-49	8.6	761	0.475	0.095	4.598	0.9789	3.859	
-50	6.5	763	0.49	0.098	4.588	0.9787	3.847	
-51	4.1	758	0.665	0.133	4.575	0.9709	3.535	
-52	3	760	2.175	0.435	4.607	0.9421	2.850	
C_3-53	11	761	0.43	0.086	4.598	0.9813	3.438	
-54	8.6	761	0.453	0.0906	4.599	0.980	3.954	
-55	6.5	763	0.49	0.098	4.588	0.9787	3.847	
-56	4.1	765	0.62	0.124	4.575	0.9738	3.64	
-57	3	760	0.645	0.129	4.606	0.9720	3.575	
Nitrogen Flow Rate = 75 cc. per min.								
C_1-58	11	765	1.855	0.372	4.575	0.9761	3.73	0.2686
-59	8.6	765	1.89	0.378	4.574	0.9739	3.665	0.2679
-60	6.5	768	2.11	0.422	4.557	0.9632	3.30	0.264
-61	4.1	769	2.18	0.436	4.551	0.959	3.21	0.263
-62	3	764	2.25	0.448	4.605	0.9575	3.31	0.266

Run No.	1	2	3	4	5	6	7	$y^* \times 10^2$
z_2-63	11	764	0.54	0.108	4.574	0.9763	3.746	
-64	8.6	764	0.58	0.116	4.574	0.9746	3.77	
-65	6.5	768	0.676	0.1351	4.567	0.970	3.51	
-66	4.1	769	0.705	0.141	4.552	0.9690	3.47	
-67	3	764	0.840	0.168	4.605	0.9635	3.32	
z_3-68	11	765	0.48	0.096	4.551	0.9789	3.86	
-69	8.6	769	0.511	0.1022	4.575	0.9771	3.77	
-70	6.5	768	0.621	0.124	4.557	0.9726	3.61	
-71	4.1	769	0.65	0.130	4.552	0.9715	3.42	
-72	3	764	0.746	0.149	4.580	0.9674	3.42	
Nitrogen Flow Rate = 100 cc. per min.								
z_1-73	11	769	1.98	0.397	4.551	0.9893	4.53	0.352
-74	8.6	769	2.05	0.410	4.551	0.9855	4.26	0.351
-75	6.5	772	2.47	0.494	4.535	0.9640	3.325	0.344
-76	4.1	773	2.545	0.509	4.526	0.959	3.20	0.336
-77	3	768	2.55	0.510	4.556	0.960	3.04	0.344
z_2-78	11	769	0.805	0.161	4.551	0.9646	3.34	
-79	8.6	769	0.86	0.172	4.551	0.9642	3.27	
-80	6.5	772	0.945	0.189	4.534	0.9583	3.175	
-81	4.1	773	0.965	0.193	4.526	0.957	3.15	
-82	3	768	1.095	0.2126	4.556	0.951	3.23	
z_3-83	11	769	0.745	0.149	4.551	0.967	3.38	
-84	8.6	769	0.785	0.158	4.551	0.9655	3.365	
-85	6.5	772	0.855	0.171	4.534	0.9622	3.525	
-86	4.1	773	0.8925	0.1785	4.552	0.9607	3.24	
-87	3	768	0.98	0.1925	4.551	0.9577	3.17	

TABLE 1-6

I.D. of Slug Flow Absorber = 0.6 cm.
Nitrogen Flow Rate = 50 cc. per min.
Top Loading.

Run No.	1	2	3	4	5	6	7	$y^* \times 10^2$
C_1-88	11	762	1.23	0.246	4.591	0.9859	4.26	0.1838
-89	8.9	762	1.295	0.259	4.594	0.9830	4.072	0.1838
-90	7	764	1.413	0.283	4.579	0.9775	3.79	0.1838
-91	4.9	764	1.49	0.299	4.583	0.9740	3.645	0.1838
-92	3.2	762	1.49	0.300	4.593	0.9742	3.654	0.1838
C_2-93	11	762	0.40	0.080	4.591	0.9826	4.052	
-94	8.9	762	0.4625	0.0925	4.594	0.980	3.90	
-95	7	764	0.595	0.102	4.579	0.9782	3.8545	
-96	4.9	763.7	0.51	0.100	4.583	0.9775	3.80	
-97	3.2	762	0.53	0.104	4.593	0.9770	3.77	
C_3-98	11	762	0.35	0.070	4.591	0.9850	4.20	
-99	8.9	762	0.44	0.088	4.594	0.9808	3.953	
-100	7	764	0.465	0.094	4.579	0.9795	3.88	
-101	4.9	764	0.49	0.098	4.583	0.9786	3.845	
-102	3.2	762	0.50	0.10	4.593	0.9782	3.827	
Nitrogen Flow Rate = 75 cc. per min.								
C_1-103	11	765	1.65	0.33	4.575	0.9854	4.227	0.2673
-104	8.9	766	1.695	0.339	4.570	0.9836	4.111	0.2673
-105	7	768	1.825	0.375	4.555	0.979	3.89	0.2673
-106	4.9	768	1.880	0.376	4.535	0.9740	3.65	0.2673
-107	3.2	766	1.90	0.380	4.569	0.9752	3.69	0.2673

un o.	1	2	3	4	5	6	7	$y^* \times 10^2$
2 -108	11	765	0.545	0.109	4.575	0.9761	3.736	
-109	8.9	766	0.5425	0.1085	4.570	0.9763	3.74	
-110	7	768	0.575	0.115	4.555	0.9748	3.675	
-111	4.9	768	0.578	0.1155	4.559	0.9746	3.67	
-112	3.2	766	0.58	0.1155	4.569	0.9747	3.675	
3 -113	11	765	0.46	0.092	4.575	0.9780	3.905	
-114	8.9	766	0.465	0.093	4.570	0.9797	3.89	
-115	7	768	0.510	0.101	4.555	0.9777	3.80	
-116	4.9	768	0.523	0.105	4.559	0.9770	3.79	
-117	3.2	766	0.518	0.104	4.569	0.9774	3.79	
itrogen Flow Rate = 100 cc. per min.								
1 -118	11	767	2.10	0.420	4.560	0.9825	4.05	0.3488
-119	8.9	772	2.18	0.436	4.532	0.979	3.87	0.3488
-120	7	772	2.155	0.431	4.534	0.9804	3.925	0.3488
-121	4.9	772	2.16	0.432	4.535	0.9804	3.90	0.3488
-122	3.2	770	2.27	0.454	4.545	0.9749	3.68	0.3488
2 -123	11	767	0.73	0.146	4.561	0.9680	3.44	
-124	8.9	772	0.755	0.151	4.532	0.9667	3.40	
-125	7	772	0.765	0.153	4.534	0.9663	3.388	
-126	4.9	772	0.775	0.155	4.535	0.9665	3.37	
-127	3.2	772	0.830	0.166	4.545	0.9635	3.31	
3 -128	11	769	0.630	0.127	4.560	0.9722	3.58	
-129	8.9	772	0.643	0.132	4.532	0.9717	3.55	
-130	7	772	0.68	0.134	4.	0.9705	3.52	
-131	4.9	772	0.69	0.138	4.535	0.9696	3.49	
-132	3.2	772	0.74	0.148	4.545	0.9674	3.42	

TABLE 1-7

.D. of Slug Flow Absorber = 0.4 cm.
itrogen Flow Rate = 50 cc. per min.
ottom Loading

un o.	1	2	3	4	5	6	7	$y^* \times 10^2$
1 -1	12.8	767	1.49	0.296	4.563	0.9735	3.630	0.1823
-2	9.65	764	1.505	0.301	4.579	0.9731	3.615	0.1828
-3	7.25	771	1.535	0.3075	4.542	0.9710	3.537	0.1809
-4	5.05	771	1.59	0.318	4.543	0.9685	3.45	0.1808
-5	3	768	1.84	0.368	4.559	0.9570	3.147	0.179
2 -6	12.8	767	0.5525	0.1105	4.563	0.9759	3.722	
-7	9.65	764	0.568	0.114	4.579	0.9752	3.69	
-8	7.25	771	0.54	0.108	4.542	0.9763	3.741	
-9	5.05	771	0.635	0.129	4.543	0.9716	3.562	
-10	3	768	0.86	0.174	4.559	0.9620	3.27	
3 -11	12.8	767	0.495	0.098	4.563	0.9783	3.83	
-12	9.65	757	0.50	0.10	4.579	0.9782	3.83	
-13	7.25	771	0.51	0.102	4.541	0.9775	3.795	
-14	5.05	771	0.585	0.117	4.543	0.9743	3.659	
-15	3	768	0.768	0.154	4.560	0.9669	3.39	

itrogen Flow Rate = 75 cc. per min.

1 -16	12.8	771	2.02	0.404	4.539	0.9673	3.42	0.2642
-17	9.65	768	2.138	0.428	4.556	0.9618	3.26	0.2638
-18	7.25	775	2.165	0.433	4.519	0.9595	3.20	0.2610
-19	5.05	774	2.155	0.431	4.520	0.960	3.22	0.2609

Run No.	1	2	3	4	5	6	7	$y^* \times 10^2$
z_1 -20	3	772	2.81	0.562	4.535	0.960	2.69	0.2537
z_2 -21	12.8	771	0.7225	0.1445	4.539	0.9682	3.45	
-22	9.65	768	0.736	0.1472	4.556	0.9678	3.431	
-23	7.25	775	0.775	0.156	4.519	0.9657	3.363	
-24	5.05	774	0.75	0.15	4.520	0.9668	3.405	
-25	3	772	1.373	0.275	4.536	0.9395	2.815	
z_3 -26	12.8	771	0.655	0.131	4.539	0.9712	3.54	
-27	9.65	768	0.68	0.134	4.556	0.9706	3.55	
-28	7.25	775	0.695	0.139	4.519	0.9693	3.48	
-29	5.05	774	0.68	0.137	4.520	0.9695	3.49	
-30	3	772	1.19	0.237	4.536	0.9488	2.950	
Nitrogen Flow Rate = 100 cc. per min.								
z_1 -31	12.8	774	2.39	0.479	4.521	0.9673	3.32	0.3427
-32	9.65	773	2.433	0.487	4.533	0.9658	3.38	0.344
-33	7.25	779	2.645	0.533	4.495	0.9534	3.195	0.336
-34	5.05	778	2.73	0.546	4.496	0.949	3.00	0.335
-35	3	776	3.80	0.760	4.510	0.8945	2.25	0.3177
z_2 -36	12.8	774	0.8075	0.162	4.522	0.9643	3.33	
-37	9.65	772	0.81	0.162	4.533	0.9643	2.98	
-38	7.25	779	0.868	0.174	4.495	0.9614	3.26	
-39	5.05	778	1.02	0.203	4.496	0.9548	3.10	
-40	3	776	1.90	0.380	4.511	0.9156	2.47	
z_3 -41	12.8	774	0.715	0.143	4.522	0.9684	3.45	
-42	9.65	772	0.695	0.139	4.556	0.9695	3.485	
-43	7.25	779	0.713	0.143	4.496	0.9683	3.45	
-44	5.05	778	0.89	0.178	4.496	0.960	3.23	
-45	3	776	1.60	0.320	4.451	0.930	2.66	

TABLE 1-8

D. of Slug Flow Absorber = 0.5 cm.
itrogen Flow Rate = 50 cc. per min.

un o.	1	2	3	4	5	6	7	$y^* \times 10^2$
1 -46	12	770	1.44	0.288	4.548	0.9758	3.72	0.181
-47	9.2	761	1.51	0.302	4.599	0.9732	3.630	0.184
-48	7.3	764	1.59	0.317	4.584	0.9694	3.485	0.1823
-49	5.5	762	1.61	0.322	4.594	0.9683	3.45	0.1826
-50	3	770	1.68	0.336	4.543	0.9639	3.31	0.179
2 -51	12	770	0.44	0.088	4.548	0.9807	3.945	
-52	9.2	761	0.477	0.0955	4.598	0.9792	3.873	
-53	7.3	764	0.49	0.099	4.584	0.9785	3.840	
-54	5.5	762	0.518	0.104	4.592	0.9773	3.78	
-55	3	770	0.54	0.108	4.543	0.9762	3.74	
3 -56	12	770	0.373	0.075	4.548	0.9789	4.11	
-57	9.2	761	0.393	0.079	4.598	0.9830	4.073	
-58	7.3	764	0.415	0.083	4.586	0.9819	4.012	
-59	5.5	762	0.43	0.086	4.589	0.9804	3.93	
-60	3	770	0.455	0.091	4.543	0.980	3.913	

itrogen Flow Rate = 75 cc. per min.

1 -61	12	774	2.155	0.431	4.525	0.960	3.22	0.26
-62	9.2	765	2.1625	0.4325	4.574	0.9610	3.24	0.265
-63	7.3	767	2.183	0.437	4.562	0.959	3.21	0.266
-64	5.5	768	2.195	0.439	4.558	0.9591	3.19	0.2635
-65	3	774	2.51	0.50	4.519	0.9435	2.87	0.261
2 -66	12	774	0.655	0.1311	4.525	0.9711	3.555	

Run No.	1	2	3	4	5	6	7	$y^* \times 10^2$
2 -67	9.2	765	0.668	0.134	4.574	0.9708	3.535	
-68	7.3	767	0.673	0.135	4.562	0.9705	3.522	
-69	5.5	768	0.693	0.1396	4.558	0.9696	3.49	
-70	3	773	0.81	0.162	4.527	0.9670	3.33	
3 -71	12	766	0.555	0.111	4.568	0.9758	3.715	
-72	9.2	765	0.55	0.115	4.575	0.9749	3.69	
-73	7.3	767	0.55	0.109	4.563	0.9761	3.74	
-74	5.5	768	0.583	0.117	4.558	0.9745	3.66	
-75	3	774	0.625	0.125	4.528	0.9722	3.58	
Nitrogen Flow Rate = 100 cc. per min.								
1 -76	12	778	2.275	0.455	4.501	0.9730	3.61	0.343
-77	9.2	769	2.377	0.476	4.551	0.9687	3.465	0.343
-78	7.3	771	2.39	0.478	4.539	0.969	3.435	0.334
-79	5.5	772	2.43	0.486	4.535	0.966	3.46	0.356
-80	3	777	2.83	0.564	4.504	0.9454	3.00	0.334
2 -81	12	778	0.71	0.142	4.502	0.9685	3.457	
-82	9.2	769	0.79	0.158	4.551	0.9653	3.3617	
-83	7.3	771	0.815	0.163	4.539	0.9686	3.32	
-84	5.5	764	0.805	0.161	4.535	0.9645	3.34	
-85	3	777	1.025	0.205	4.504	0.9545	3.09	
3 -86	12	778	0.60	0.119	4.502	0.9735	3.63	
-87	9.2	769	0.675	0.135	4.551	0.970	3.51	
-88	7.3	771	0.69	0.138	4.539	0.9641	3.49	
-89	5.5	772	0.685	0.137	4.535	0.970	3.50	
-90	3	777	0.82	0.168	4.504	0.9631	3.313	

TABLE 1-9

.D. of Bottom Loading Slug Flow Absorber = 0.6 cm.
litrogen Flow Rate = 50 cc. per min.

Run No.	1	2	3	4	5	6	7	$y^* \times 10^2$
z_1 -91	10	767	1.085	0.217	4.551	0.9926	4.92	0.185
-92	8.1	767	1.15	0.227	4.566	0.9896	4.57	0.185
-93	5.9	763	1.19	0.238	4.587	0.9882	4.43	0.1857
-94	4.6	765	1.19	0.238	4.578	0.9880	4.39	0.1853
-95	3.2	766	1.205	0.241	4.570	0.9873	4.37	0.1849
z_2 -96	10	769	0,288	0.058	4.551	0.9874	4.38	
-97	8.1	767	0.323	0.065	4.566	0.9859	4.26	
-98	5.9	763	0.348	0.073	4.587	0.9848	4.19	
-99	4.6	765	0.39	0.079	4.578	0.9827	4.05	
-100	3.2	766	0.408	0.082	4.570	0.9821	4.02	
z_3 -101	10	767	0.23	0.046	4.551	0.990	4.58	
-102	8.1	767	0.253	0.0506	4.566	0.9889	4.50	
-103	5.9	763	0.255	0.051	4.587	0.9889	4.49	
-104	4.6	765	0.357	0.072	4.578	0.9844	4.16	
-105	3.2	766	0.348	0.0695	4.570	0.9848	4.09	

litrogen Flow Rate = 75 cc. per min.

z_1 -106	10	773	1.48	0.29	4.531	0.9863	4.75	0.27
-107	8.1	769	1.575	0.315	4.554	0.9895	4.44	0.27
-108	5.9	767	1.60	0.32	4.563	0.9885	4.46	0.2707
-109	4.6	773	1.655	0.331	4.526	0.9851	4.20	0.2671
-110	3.2	766	1.748	0.3496	4.636	0.9850	4.83	0.274

Run No.	1	2	3	4	5	6	7	$y^* \times 10^2$
C_2-111	10	773	0.50	0.10	4.531	0.9780	3.818	
-112	8.1	769	0.533	0.107	4.556	0.9764	3.76	
-113	5.9	767	0.559	0.112	4.563	0.9748	3.71	
-114	4.6	773	0.57	0.126	4.526	0.9748	3.675	
-115	3.2	766	0.668	0.132	4.636	0.9730	3.56	
C_3-116	10	773	0.44	0.088	4.531	0.9806	4.05	
-117	8.1	769	0.465	0.088	4.554	0.9806	3.94	
-118	5.9	767	0.475	0.095	4.556	0.9788	3.86	
-119	4.6	773	0.58	0.10	4.526	0.9792	3.85	
-120	3.2	766	0.568	0.113	4.636	0.9757	3.71	
Nitrogen Flow Rate = 100 cc. per min.								
C_1-121	10	777	1.80	0.361	4.507	0.9974	5.52	0.3509
-122	8.1	772	1.853	0.370	4.532	0.9953	5.38	0.3523
-123	5.9	772	1.920	0.384	4.535	0.9922	4.85	0.3514
-124	4.6	777	1.934	0.402	4.506	0.9918	4.85	0.3488
-125	3.2	767	2.177	0.435	4.728	0.9837	4.11	0.364
C_2-126	10	777	0.51	0.118	4.507	0.9738	3.77	
-127	8.1	772	0.626	0.125	4.554	0.9723	3.58	
-128	5.9	772	0.635	0.127	4.535	0.9720	3.57	
-129	4.6	777	0.635	0.127	4.506	0.9718	3.569	
-130	3.2	767	0.8825	0.178	4.728	0.9622	3.275	
C_3-131	10	777	0.485	0.097	4.508	0.9785	3.82	
-132	8.1	772	0.628	0.125	4.532	0.9767	3.77	
-133	5.9	772	0.5425	0.117	4.536	0.9743	3.66	
-134	4.6	777	0.535	0.107	4.506	0.9763	3.74	
-135	3.2	767	0.78	0.156	4.728	0.9671	3.	

APPENDIX 2

Sample Calculation and Calculated Results

1. Mass Transfer Runs

Sample Calculation Run No. C_2-53

Observed Readings

Contacting length = 7.3 cm.

Potentiometer reading = 0.49 M. V.

Experimental temperature = 22° C.

Saturator temperature = - 4° C.

Flowmeter reading = 6.3

Manometer pressure = 7 mm. Hg.

Atmospheric pressure = 757 mm. Hg.

Bubble Size

Bubble length = 0.724 cm.

Surface area = 1.36 $cm.^2$ (Table 2-3)

Volume = 0.18 $cm.^3$ (Table 2-3)

Time of Rise

Velocity of rise = 7.3 cc./sec.

Actual height of rise = 7.3 - 0.70 = 6.6 cm.

Time of rise = $\frac{6.576}{7.3}$ = 0.91 sec.

Total Efficiencies

Concentration of n-hexane in exit gas stream (Table 1-8) = 0.099%

Concentration of n-hexane in inlet gas stream

Saturated at - 4° C. = $\frac{35.00}{757 + 7}$ x 100% = 4.584%

Total efficiency $E_T = \frac{y_{on} - y_{off}}{y_{on}} = \frac{0.04584 - 0.00094}{0.04584}$

$= 0.9785$

and $- \ln (1 - E_T) = 3.840$

Mass Transfer Coefficient, K_{OG}

$$K_{OG} = \frac{\text{Slope} \times G}{P \times A \times f}$$

Slope = 0.53 (Table 2-4)

G = 3.487×10^{-5} g-mole/sec.

P = 1 atm

A = 1.36 $cm.^2$ (Table 2-3)

f = 4.68 bubbles/sec. (Table 2-4)

K_{OG} = 0.029×10^{-4} g-mole/atm. $cm.^2$ sec.

TABLE 2-1

Mass Transfer Coefficient, K_{OG}, in Wetted Wall Column

N_2 Flow rate cc./min.	I.D. cm.	Molal gas Flow rate (g-mole/sec.) x 10^5	Cross-section Area $cm.^2$	Atm. Pressure atm.	Slope of $-\ln(1-E)$ vs Θ	Velocity cm./sec.	$K_{OG} = \frac{\text{Slope} \times G}{PAV}$ (g-mole/atm. sec. $cm.^2$) x 10^4
50	0.4	3.48	0.365	1	6.4	8.13	0.23
75	0.4	5.23	0.365	1	5.9	12.20	0.22
100	0.4	6.97	0.365	1	6.22	16.3	0.23
50	0.5	3.48	0.468	1	3.08	5.0	0.15
75	0.5	5.23	0.468	1	3.33	7.4	0.16
100	0.5	6.97	0.468	1	3.50	10.0	0.17

Evaluation of Bubble Diameter and Bubble Rising Velocity Using Equations Recommended by Hobler (32)

Equations :

Bubble diameter : $d = 0.943\ V^{0.4}$ m for turbulent flow ..... (a)

Rising velocity : $W = \sqrt{\frac{dg}{2}}$ cm./sec. for turbulent flow ..... (b)

Reynold No. : $\frac{W \rho_g d}{\eta_g} = Re$ ..... (c)

Critical rate of flow : $V_c = \frac{\pi W}{6} \left(\frac{6D\sigma}{\gamma_g - \gamma_g} \right)^{2/3}$ $cm.^2$/sec. .... (d)

$$\bar{\gamma}_\ell = \rho_\ell \cdot \bar{g}/g = 0.751 \text{ g (force)/cm.}^3$$

$$\bar{\gamma}_g = \rho_g \cdot \bar{g}/g = 0.0015 \text{ g (force)/cm.}^3$$

As volumetric flow rates employed were greater than their corresponding critical values calculated with equation (d), the flows were therefore all chain like flow. The flow rates were also found to be turbulent using equation (c).

TABLE 2-2

Mass Transfer Coefficient

N_2 Flow rate cc./min.	Molal Gas Flow Rate, G. (g-mole/sec.) x 10^5	Bubble Diameter d, cm.	Surface Area, A $cm.^2$	Frequency, f Bubbles/sec.	Slope of $-\ln(1-E_T)$ vs Θ	$K_{OG} = \frac{\text{Slope} \times G}{P A f}$ (g-mole/sec. $cm.^2$ atm) x 10^4
50	3.48	0.36	0.398	37.1	14.7	0.35
75	5.23	0.42	0.55	34	14.4	0.40
100	6.97	0.47	0.69	32	13.7	0.43

TABLE 2-3

Determination of Surface Area and Volume of Bubbles in Slug Flow Absorber

The volume and surface area of the bubbles were obtained by dividing each bubble into three different parts and measuring directly

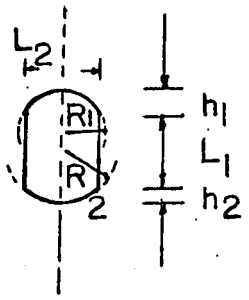

Sketch of a rising bubble in 0.5 cm. I. D. slug flow absorber

From Photograph

L_1 = 1 cm. L_2 = 0.95 cm. = 2R

h_1 = 0.32 cm. h_2 = 0.2 cm.

$2R_1$ = 1.15 cm. $2R_2$ = 2.84 cm.

Scale factor = 0.4761

Standard Formula Used

Volume of the spherical segment of the bubble = $V = \frac{\pi h^2}{3}(2R - h)$

Surface area of the spherical segment of the bubble = $A = 2\pi Rh$

$$\text{Total volume of the bubble} = \frac{\pi h_1}{3}(2R_1 - h_1) + \pi\left(\frac{L_2}{2}\right)^2 L_1 + \frac{\pi h_2}{3}(2R_2 - h_2)$$

$$= 0.0095 + 0.17 + 0.012$$

$$= 0.182 \text{ cm.}^3$$

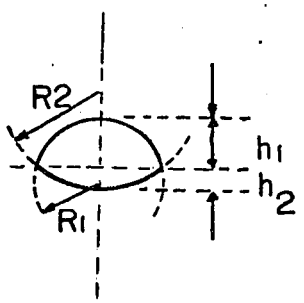

Sketch of a rising bubble in 0.6 cm. I.D. slug flow absorber

From Photograph

h_1 = 0.25 cm., h_2 = 0.15 cm.

$2R_1$ = 0.9 cm., $2R_2$ = 1.75 cm.

Scale factor = 1.052

Actual Size

h_1 = 0.26 cm., h_2 = 0.16 cm.

$2R_1$ = 0.95 cm., $2R_2$ = 1.84 cm.

$$\text{Total volume of the bubble} = \frac{\pi h_1}{3}(2R_1 - h_1) + \frac{\pi h_2}{3}(2R_2 - h_2)$$

$$= 0.0495 + 0.044$$

$$= 0.094 \text{ cm.}^3$$

$$\text{Surface area of the bubble} = 2\pi R_1 h_1 + 2\pi R_2 h_2$$

$$= 0.9132 + 0.7829$$

$$= 1.70 \text{ cm.}^2$$

TABLE 2-4

Contact Time and Mass-Transfer Coefficient in Slug Flow Absorber

N_2 Flow Rate = 50 cc./min.

Molal Gas Flow Rate, G = 3.5×10^{-5} g-mole/sec.

Run No.	I. D. cm.	Contacting Length cm.	Bubble Length cm.	Actual length of rise cm.	Contact Time Θ, sec.	Frequency, f bubbles/sec.	$-\ln(1-E_T)$ vs Θ	$K_{OG} = \frac{\text{Slope } G}{f_s P A_S}$ (g-mole/atm. cm.^{2} sec.) $\times 10^4$
C_2-51	0.5	12	0.72	11.3	1.545	4.7	0.53	0.029
-52	0.5	9.2	0.72	8.5	1.16	4.7	0.53	0.029
-53	0.5	7.3	0.72	6.6	0.90	4.7	0.53	0.029
-54	0.5	5.5	0.72	4.8	0.64	4.7	0.53	0.029
-55	0.5	3	0.72	2.3	0.31	4.7	0.53	0.029
C_2-96	0.6	10	0.42	9.6	1.49	9.1	0.1	0.025
-97	0.6	8.1	0.42	7.7	1.19	9.1	0.1	0.025
-98	0.6	5.9	0.42	5.5	0.86	9.1	0.1	0.025
-99	0.6	4.6	0.42	4.2	0.65	9.1	0.1	0.025
-100	0.6	3.2	0.42	2.7	0.43	9.1	0.1	0.025

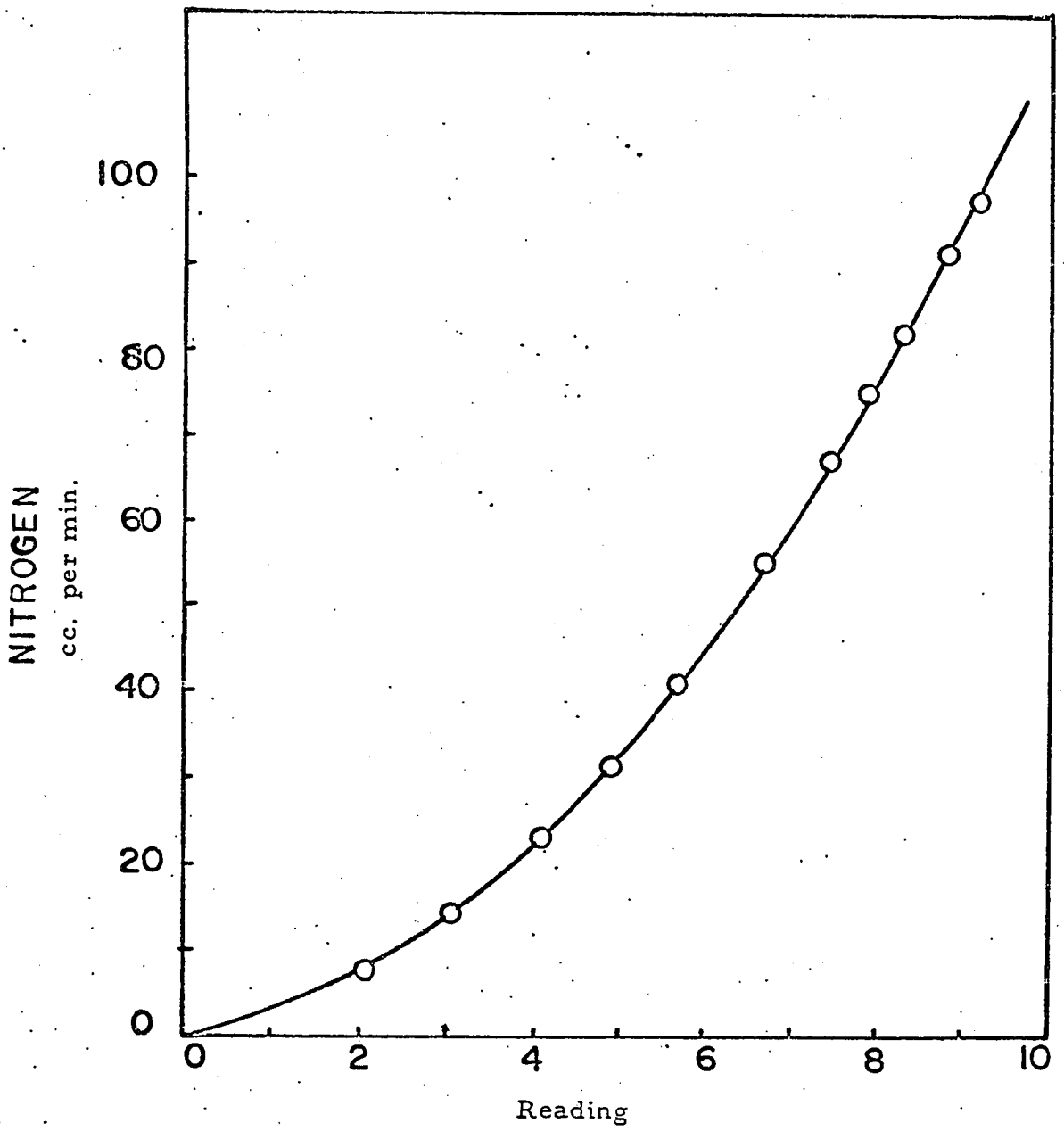

Figure 21: Calibration Curve of Flowmeter.